

Dear Editor Peter Haynes,

we have addressed the reviewer's comments and believe that the manuscript has improved thanks to their suggestions. Most important, we have addressed the issue of the seasonal variations of the ODP-weighted emissions by adding a Figure to the Supplement (S1) and some text to the discussions of Figure 4 and Figure 6. We have changed the manuscript according to the editorial comments of the reviewers and think that these changes have improved the presentation quality of the manuscript. In a few places we have shortened the text to condense the manuscript.

We will submit the manuscript with bold face and crossed-out font indicating where the text has been changed. Please let us know if you find our suggestion acceptable and agree with this as the final version of the paper. Thanks a lot for your help throughout the review process.

Sincerely, Susann Tegtmeier

Anonymous Referee #1

Tegtmeier et al presents a quantitative estimate of the ozone depletion potential (ODP)-weighted emission calculation for the most abundant very-short-lived brominated compound, CHBr₃. The revised manuscript has taken serious consideration of the comments given by the previous reviewers and has addressed several major concerns raised by the two reviewers. My comments are mainly editorial, but this likely is not a full list of needed corrections. I would recommend (i) the authors seek some editorial help from a native English speaker or the ACP editorial office; (ii) the manuscript is very long and can use some condensing.

We thank Referee 1 for his/her valuable comments. We have changed the manuscript according to the comments listed below. We think that these changes have improved the presentation quality of the manuscript. In a very few cases we have decided to use a slightly different sentence than suggested by the reviewer as pointed out by our response given in italic.

Minor comments:

L61: “coupled to” -> due to

L69: 21 -> 21st

L83: troposphere-to-stratosphere transport

L86: “it remains ... climate” -> the role of oceanic VSLS on stratospheric ozone in a future changing climate remains a challenge.

We have changed the sentence to “While stratospheric ozone depletion due to long-lived halocarbons is expected to level off and reverse (Austin and Butchart, 2003), assessing oceanic VSLS and their impact on stratospheric ozone in a future changing climate remains a challenge.”

L92-95: Sounds awkward. Consider rephrasing.

We have changed the sentence to “The current best-estimate range of 2-8 ppt (Carpenter and Reimann et al., 2014) includes observation-derived estimates of 2.9 ppt (Sala et al., 2014) and model-derived estimates of 4 ppt (Hossaini et al., 2013), 4.5-6 ppt (Aschmann and Sinnhuber, 2013) and 7.7 ppt (Liang et al., 2014).”

L98-100: Change to “The resulted change in O₃ leads to a contribution of -0.02 Wm⁻² to global radiative forcing.

L105-106: troposphere-to-stratosphere transport

L119: delete “,” after anthropogenic

L126: Change to “As a consequence,”

L128: Delete “So far”

L140-141: Change to “will require weighting emissions and ODPS, both are highly variable”

We have changed the sentence to “For the VSLS, however, the concept of ODP-weighted emissions has not yet been applied. To do so requires combining estimates of the emissions with the ODPS, both of which are highly variable in space and time”.

- L144: delete “the” before CHBr₃
- L145: add “,” after framework
- L146: “allow to compare” -> comparison of
- L208: Delete “by” before changes
- L211: Delete “oceanic”
- L218: You should probably cite Wuebbles et al. (1983) here.
- L241: trajectories -> trajectory
- L308-312: Change to “We expect changes in the stratospheric residence time only have small impact on the future ODP, compared to the impacts of tropospheric transport and stratospheric chemistry.
- L423: Change “the ones of human-made” to “the manmade”
- L427: Change to “less than 10% of the regions over the globe”
- L432: “Already this lower boundary of the” -> Even the lower limit of the; delete “,” after emissions.
- L433: Delete “even”
We have decided to delete the whole sentence in line 432 and keep the word ‘even’ in line 433.
- L436: Delete “even”
- L436-438: -> The CHBr₃ emissions and ODP show similar latitudinal ...
- L439: causes -> leads to
- L481: add “the” before strongest
- L488: -> To analyze the future change of ODP-weighted CHBr₃ emissions, we need to extend the times series beyond 2006.
We have changed the sentence to “In oder to analyze the long-term changes of ODP-weighted CHBr₃ emissions, we need to extend the time series beyond the 1999-2006 time period.”
- L496: south-east -> Southeast
- L511: south-east ward pointing -> southeastward
- L556-558: Is the seasonal cycle mainly driven by seasonality in deep convection or emissions, or both?
Indeed the seasonal cycle is driven by a combination of the seasonality in emissions and deep convection. To make this clear we have added a figure of the CHBr₃ emissions for the months June and December to the Supplement.
We have added the text “The emissions reveal some seasonal variations which are most apparent in the Indian Ocean with peak values during NH summer along the equator and along the NH coast lines (see Fig. S1 in the Supplement). Note that CHBr₃ concentrations maps represent climatological fields and the seasonal variations in the emission fields stem from varying surface winds and sea surface temperature (see Section 2.1). Global average CHBr₃ emissions show a seasonal cycle of about 25% with a peak in July and a minimum in April (Ziska et al., 2013). The seasonality of the ODP (Figure 5a) driven by the seasonality of deep convection amplifies the seasonal

variations in the emissions and thus causes the pronounced shift of the ODP-weighted emissions from one hemisphere to the other.” to the discussion of Figure 4.

Furthermore we have added the text “The same signal is evident from the CHBr₃ emissions itself (see Figure S1 in the Supplement) and is amplified by the shift of high ODP values to the NH tropics during NH summer (Figure 5a and c). The pronounced seasonal cycle of the ODP-weighted emissions indicates a seasonality of the CHBr₃ concentrations in the TTL, which needs to be verified by observations.” to the discussion of Figure 6.

L577: Delete “nevessarily”

L624: inner -> deep

L625: can reach locally higher values -> show higher local maxima

L633: delete “a” before similar

L643-644: reasonably well captured -> captured reasonably well

L644: encouraging -> lending confidence in

L698: Add “(5.4%)” after increase

L699-701: Delete the “If … simulations.” sentence.

L814: tropospheric transport -> troposphere-to-stratosphere transport

L818: 31% increase respect to what year?

Figure 3: HCFC-141 and HCFC-142 should be HCFC-141b and HCFC-142b

Anonymous Referee #2

Review 'Oceanic bromoform emissions weighted by their ozone depletion potential' by Tegtmeier et al.,

The authors have done a great job in tightening this manuscript and addressing all of my concerns raised in my first review. I only have minor comments and a clarification.

Clarification / Discussion point

The ODP-weighted CHBr₃ emissions displayed in figure 9 show a maximum in the boreal summer when mass fluxes are weaker than the austral summer ODP mass-fluxes (figure 5c). This is due (and mentioned in the paper) to the very high emissions in SA Asia, that are lacking in the MC from Ziska, 2013. However, the seasonality of emissions in these regions is not taken into account (and observations in both regions are likely to be biased to certain seasons), so a stronger caveat in the interpretation of figure 9 would add to the discussion. While differing model results support this seasonality, meaning their meteorology and mass fluxes support each other, but I assume all runs were being driven by the same Ziska emission fields – so this is not surprising. It would be useful to produce a figure 9 curve with a different emission inventory to test the robustness of this seen seasonality in ODPs. A comment about this expected seasonality in stratospheric bromoform concentrations and the requirement that this UTLS bromoform seasonality needs to be verified by observations would also add to the discussion.

The CHBr₃ emissions from Ziska et al. (2013) include seasonal and interannual variations driven by varying surface winds and sea surface temperature. The seasonal variations of the ODP-weighted emissions are driven by a combination of the seasonality in emissions and deep convection. To make this clear we have added a figure of the CHBr₃ emissions for the months June and December to the Supplement (Figure S1). Additionally, we have added the text "The emissions reveal some seasonal variations which are most apparent in the Indian Ocean with peak values during NH summer along the equator and along the NH coast lines (see Fig. S1 in the Supplement). Note that CHBr₃ concentrations maps represent climatological fields and the seasonal variations in the emission fields stem from varying surface winds and sea surface temperature (see Section 2.1). Global average CHBr₃ emissions show a seasonal cycle of about 25% with a peak in July and a minimum in April (Ziska et al., 2013). The seasonality of the ODP (Figure 5a) driven by the seasonality of deep convection amplifies the seasonal variations in the emissions and thus causes the pronounced shift of the ODP-weighted emissions from one hemisphere to the other." to the discussion of Figure 4. Furthermore we have added the text "The same signal is evident from the CHBr₃ emissions itself (see Figure S1 in the Supplement) and is amplified by the shift of high ODP values to the NH tropics during NH summer (Figure 5a and c). The pronounced seasonal cycle of the ODP-weighted emissions indicates a

seasonality of the CHBr₃ concentrations in the TTL, which needs to be verified by observations.” to the discussion of Figure 6.

Since none of the other available emission inventories includes seasonal variations, it is not possible to test the robustness of the seasonality of the ODP-weighted emissions based on an additional curve.

We thank Referee 1 for his/her valuable comments. We have changed the manuscript according to all comments listed below. We think that these changes have improved the presentation quality of the manuscript.

Minor Typos / Grammatical changes

Line 74 – ‘however evidence arises’ change to ‘however evidence has emerged’

Line 99 change to: Through the relatively large impact of VSLs on ozone in the lower stratosphere, VSLs contribute -0.02 Wm-2 to global radiative forcing (~6% of the 0.33 Wm-2 from all ODS halocarbons) ...

Line 106 compared change to relative

Line 120 measure change to metric

Line 125 change to only a fraction of the originally released VSLs reaches the...

Line 126 change ‘cannot be given’ as to ‘is not’

Line 140 will require change to requires

Line 144 remove will

Line 146 ‘will allow to compare’ change to ‘allows assessment of’

Line 155 change which takes to taking

Line 208 remove by after the

Line 210 add s to increase

Line 311 change cost-efficient to computationally-efficient

Line 687 change ‘global warming’ to ‘increased GHG induced tropospheric warming’ leading to

Line 745 change ‘a particular high’ to ‘particularly high’

Line 746 change from to due to

Line 751 change to lead to a two to three-fold increase in ODP-weighted ...

1 **Oceanic bromoform emissions weighted by their ozone depletion potential**

2

3

4 **S. Tegtmeier¹, F. Ziska¹, I. Pisso², B. Quack¹, G. J. M. Velders³, X. Yang⁴, and K.**
5 **Krüger⁵**

6

7

8 ¹GEOMAR Helmholtz Centre for Ocean Research Kiel, Kiel, Germany

9

10 ²Norwegian Institute for Air Research (NILU), Kjeller, Norway

11

12 ³National Institute for Public Health and the Environment, Bilthoven, the Netherlands

13

14 ⁴British Antarctic Survey, Cambridge, UK

15

16 ⁵University of Oslo, Oslo, Norway

17

18

19

20

21

22

23

24

25

26

27

28

29

30

31 **Abstract**

32

33 At present, anthropogenic halogens and oceanic emissions of Very Short-Lived Substances
34 (VSLS) both contribute to the observed stratospheric ozone depletion. Emissions of the long-
35 lived anthropogenic halogens have been reduced and are currently declining, whereas
36 emissions of the biogenic VSLS are expected to increase in future climate due to
37 anthropogenic activities affecting oceanic production and emissions. Here, we introduce a
38 new approach of assessing the impact of oceanic halocarbons on stratospheric ozone by
39 calculating their Ozone Depletion Potential (ODP)-weighted emissions. Seasonally and
40 spatially dependent, global distributions are derived within a case-study framework for CHBr₃
41 for the period 1999 - 2006. At present, ODP-weighted emissions of CHBr₃ amount up to 50%
42 of ODP-weighted anthropogenic emissions of CFC-11 and to 9% of all long-lived ozone
43 depleting halogens. The ODP-weighted emissions are large where strong oceanic emissions
44 coincide with high-reaching convective activity and show pronounced peaks at the equator
45 and the coasts with largest contributions from the Maritime Continent and West Pacific.
46 Variations of tropical convective activity lead to seasonal shifts in the spatial distribution of
47 the ODP with the updraught mass flux explaining 71% of the variance of the ODP
48 distribution. Future climate projections based on the RCP 8.5 scenario suggest a 31% increase
49 of the ODP-weighted CHBr₃ emissions until 2100 compared to present values. This increase
50 is related to a larger convective updraught mass flux in the upper troposphere and increasing
51 emissions in a future climate. However, at the same time, it is reduced by less effective
52 bromine-related ozone depletion ~~coupled~~ **due** to declining stratospheric chlorine
53 concentrations. The comparison of the ODP-weighted emissions of short and long-lived
54 halocarbons provides a new concept for assessing the overall impact of oceanic halocarbon
55 emissions on stratospheric ozone depletion for current conditions and future projections.

56

57 **1 Introduction**

58

59 The overall abundance of ozone-depleting substances in the atmosphere has been decreasing
60 since the beginning of the ~~24~~ **21st** century as a result of the successful implementation of the
61 1987 Montreal Protocol and its later Adjustments and Amendments (**Carpenter and**
62 **Reimann et al., 2014** ~~Montzka et al., 2011~~). In contrast to the long-lived halocarbons, the
63 halogenated Very Short-Lived Substances (VSLS) with chemical lifetimes of less than 6
64 months are not controlled by the Montreal Protocol and are even suggested to increase in the

future (Hepach et al., 2014; Hossaini et al., 2015). Brominated VSLS are known to have large natural sources; however evidence arises **has emerged** that their oceanic production and emissions are enhanced through anthropogenic activities which are expected to increase in the future (Leedham et al., 2013; Ziska et al., in prep.). At present, oceanic VSLS provide a significant contribution to the stratospheric bromine budget (Carpenter and Reimann et al., 2014). In the future, the decline of anthropogenic chlorine and bromine will further increase the relative impact of oceanic VSLS on stratospheric chemistry. The absolute amount of bromine-related ozone loss, on the other hand, is expected to decrease due to decreasing stratospheric chlorine concentrations and thus a less efficient BrO/ClO ozone loss cycle (Yang et al., 2014). Furthermore, the impacts of climate change on surface emissions, troposphere-to-stratosphere transport, stratospheric chemistry and residence time will change the role of VSLS (Pyle et al., 2007; Hossaini et al., 2012). While stratospheric ozone depletion due to long-lived halocarbons is expected to level off and reverse (Austin and Butchart, 2003), **assessing oceanic VSLS and their impact on stratospheric ozone in a future changing climate remains a challenge.**

Over the last years there has been increasing evidence from observational (e.g., Dorf et al., 2006, Sioris et al., 2006) and modelling (e.g., Warwick et al. 2006, Liang et al., 2010; Tegtmeier et al., 2012) studies that VSLS provide a significant contribution to stratospheric total bromine (Br_y). Previous The **current** best-estimate range of 2-8 ppt (Montzka et al., 2011-Carpenter and Reimann et al., 2014) recently seem to converge to a slightly narrower range includes observation-derived estimates of 2.9 ppt (Sala et al., 2014) and model-derived estimates of 4 ppt (Hossaini et al., 2013), 4.5-6 ppt (Aschmann and Sinnhuber, 2013) and 7.7 ppt (Liang et al., 2014). Brominated VSLS reduce ozone in the lower stratosphere with current estimates of a 3-11% contribution to ozone depletion (Hossaini et al., 2015) or a 2-10% contribution (Braesicke et al., 2013; Yang et al., 2014). Through the relatively large impact of VSLS on ozone in the lower stratosphere, they have a radiative effect corresponding to a contribution of VSLSs contribute -0.02 W m^{-2} to global radiative forcing (Hossaini et al., 2015) (~6% of the 0.33 Wm^{-2} from all ODS halocarbons).

The most abundant bromine containing VSLS are dibromomethane (CH_2Br_2) and bromoform (CHBr_3) with potentially important source regions in tropical, subtropical and shelf waters (Quack et al., 2007). The contribution of VSLS to stratospheric bromine in form of organic source gases or inorganic product gases depends strongly on the efficiency of troposphere-to-

99 stratosphere transport compared relative to the photochemical loss of the source gases and to
100 the wet deposition of the product gases. Uncertainties in the contribution of VSLS to
101 stratospheric halogen loading mainly result from uncertainties in the emission inventories
102 (e.g., Hossaini et al., 2013) and from uncertainties in the modeled transport and wet
103 deposition processes (e.g., Schofield et al., 2011).

104

105 The relative contribution of individual halocarbons to stratospheric ozone depletion is often
106 quantified by the Ozone Depletion Potential (ODP) defined as the time-integrated ozone
107 depletion resulting from a unit mass emission of that substance relative to the ozone depletion
108 resulting from a unit mass emission of CFC-11 (CCl_3F) (Wuebbles, 1983). Independent of the
109 total amount of the substance emitted, the ODP describes only the potential but not the actual
110 damaging effect of the substance to the ozone layer, relative to that of CFC-11. The ODP,
111 traditionally defined for anthropogenic long-lived halogens, is a well-established and
112 extensively used measure and plays an important role in the Montreal Protocol for control
113 measures metrics and reporting of emissions. Some recent studies have applied the ODP
114 concept to VSLS (e.g., Brioude et al., 2010; Pisso et al., 2010), which have also natural
115 sources. Depending on the meteorological conditions, only fractions of the originally released
116 VSLS reach only a fraction of the originally released VSLS reaches the stratosphere. As a
117 consequence, the ODP of a VSLS cannot be given as is not one number as for the long-lived
118 halocarbons but needs to be quantified as a function of time and location of emission. So far
119 ODPs of VSLS have been estimated based on Eulerian (Wuebbles et al., 2001) and
120 Lagrangian (Brioude et al., 2010; Pisso et al., 2010) studies, showing strong geographical and
121 seasonal variations, in particular within the tropics. The studies demonstrated that the ODPs
122 of VSLS are to a large degree determined by the efficiency of vertical transport from the
123 surface to the stratosphere and that uncertainties in the ODPs arise mainly from uncertainties
124 associated with the representation of convection.

125

126 Combining the emission strength and the ozone-destroying capabilities of a substance in a
127 meaningful way can be achieved by calculating the ODP-weighted emissions. For the long-
128 lived halocarbons, global ODP-weighted emissions can be calculated as the product of two
129 numbers, their mean global emissions and their ODPs (e.g., Velders et al., 2007;
130 Ravishankara et al., 2009). For the VSLS, however, the concept of ODP-weighted emissions
131 has not yet been applied. To do so requires combining estimates of the emissions with the
132 ODPs, both of which are highly variable in space and time. Among the brominated VSLS,

133 the calculation of CHBr₃ ODP-weighted emissions is now possible since global emission
134 inventories (Ziska et al., 2013) and global ODP maps (Pisso et al., 2010) became available.
135 ODP-weighted emissions will provide insight in where and when the CHBr₃ is emitted that
136 impacts stratospheric ozone. Furthermore, in a globally averaged framework, the ODP-
137 weighted emissions will allow to compare comparison of the impact of past, present and
138 future long- and short-lived halocarbon emissions. The ODP-weighted emissions for the
139 anthropogenic component of the CHBr₃ emission budget cannot be calculated, since no
140 reliable estimates of anthropogenic contributions are available at the moment. The concept is
141 introduced here for the available total emission inventory.

142

143 We compile ODP-weighted emissions of CHBr₃ in form of the seasonal and annual mean
144 distribution in order to assess the overall impact of oceanic CHBr₃ emissions on stratospheric
145 ozone. First, we introduce the new approach of calculating ODP-weighted VSLs emissions,
146 which takes taking into account the high spatial variability of oceanic emission and ODP
147 fields (Section 2). Maps and global mean values of ODP-weighted CHBr₃ emissions for
148 present day conditions are given in Section 3. The method and application are introduced for
149 CHBr₃, within a case-study framework and can be applied to all VSLs where emissions and
150 ODP are available at a spatial resolution necessary to describe their variability. In Section 4,
151 we demonstrate that ODP fields of short-lived gases can be estimated based on the convective
152 mass flux from meteorological reanalysis data and develop a proxy for the ODP of CHBr₃.
153 We use this method to derive long-term time series of ODP-weighted CHBr₃ emissions for
154 1979-2013 based on ERA-Interim data in Section 5. Model-derived ODP-weighted CHBr₃
155 emissions for present conditions are introduced in Section 6. Based on model projections of
156 climate scenarios, the future development of the ODP-weighted CHBr₃ emissions is analyzed
157 in Section 7. This approach provides a new tool for an assessment of future growing biogenic
158 VSLs and declining chlorine emissions in form of a direct comparison of the global-averaged
159 ODP-weighted emissions of short- and long-lived halocarbons.

160

161 **2 Data and methods**

162

163 **2.1 CHBr₃ emissions**

164

165 The present-day global emission scenario from Ziska et al. (2013) is a bottom-up estimate of
166 the oceanic CHBr₃ fluxes. Emissions are estimated using global surface concentration maps

167 generated from the atmospheric and oceanic in-situ measurements of the HalOcAt
168 (Halocarbons in the ocean and atmosphere) database project (<https://halocat.geomar.de>). The
169 in-situ measurements collected between 1989 and 2011 were classified based on physical and
170 biogeochemical characteristics of the ocean and atmosphere and extrapolated to a global
171 $1^\circ \times 1^\circ$ grid with the Ordinary Least Square regression technique. Based on the concentration
172 maps, the oceanic emissions were calculated with the transfer coefficient parameterization of
173 Nightingale et al. (2000) adapted to CHBr₃ (Quack and Wallace, 2003). The concentration
174 maps represent climatological fields covering the time period 1989-2011. The emissions are
175 calculated as a 6-hourly time series based on meteorological ERA-Interim data (Dee et al.,
176 2011) for 1979-2013 under the assumption that the constant concentration maps can be
177 applied to the complete time period (Ziska et al., 2013). Recent model studies showed that
178 atmospheric CHBr₃ derived from the Ziska et al. (2013) bottom-up emission inventory agrees
179 better with tropical atmospheric measurements than the other CHBr₃ model estimates derived
180 from top-down emission inventories (Hossaini et al., 2013).

181
182 Future emission estimates are calculated based on the present day (1989-2011) climatological
183 concentration maps and future estimates of global sea surface temperature, pressure, winds
184 and salinity (Ziska et al., in prep.). The meteorological parameters are model output from the
185 Community Earth System Model version 1 - Community Atmospheric Model version 5
186 (CESM1-CAM5) (Neale et al., 2010) runs based on the Representative Concentration
187 Pathways (RCP) 8.5 scenarios conducted within phase 5 of the Coupled Model
188 Intercomparison Project (CMIP5) (Taylor et al., 2012). The CESM1-CAM5 model has been
189 chosen since it provides model output for all the parameters required to calculate future VSLS
190 emissions and future ODP estimates (Section 2.2). Comparisons have shown that the global
191 emissions based on historical CESM1-CAM5 meteorological data agree well with emissions
192 based on ERA-Interim fields (Ziska et al., in prep.). For the time period 2006-2100, the global
193 monthly mean emissions are calculated based on the monthly mean meteorological input
194 parameters from CESM1-CAM5 and the fixed atmospheric and oceanic concentrations from
195 Ziska et al. (2013) following the parameterization of air-sea gas exchange coefficient from
196 Nightingale et al. (2000). The future global CHBr₃ emissions increase by about 30% until
197 2100 for the CESM1-CAM5 RCP 8.5 simulation. These derived changes of the future VSLS
198 emissions are only driven by projected changes in the meteorological and marine surface
199 parameters, in particular, the-by changes in surface wind and sea surface temperature. The
200 respective contributions of wind and temperature changes to the future emission increase can

201 vary strongly depending on the oceanic region (Ziska et al., in prep). The future emissions do
202 not take into account possible changes of the oceanic concentrations, since no reliable
203 estimates of future oceanic halocarbon production and loss processes exist so far.

204

205 **2.2 CHBr₃ trajectory-derived ODP**

206

207 The Ozone Depletion Potential is a measure of a substance's destructive effect to the ozone
208 layer relative to the reference substance CFC-11 (CCl₃F) (**Wuebbles, 1983**). ODPs of long-
209 lived halogen compounds can be calculated based on the change in total ozone per unit mass
210 emission of this compound using atmospheric chemistry-transport models. Alternatively, the
211 ODP of a long lived species *X* can be estimated by a semi-empirical approach (Solomon et al.,
212 1992):

213

$$214 \quad ODP_X = \frac{M_{CFC-11}}{M_X} \frac{\alpha n_{Br} + n_{Cl}}{3} \frac{\tau_X}{\tau_{CFC-11}} \quad (1)$$

215

216 where τ is the global atmospheric lifetime, M is the molecular weight, n is the number of
217 halogen atoms and α is the effectiveness of ozone loss by bromine relative to ozone loss by
218 chlorine. In contrast to the long-lived halocarbons, for VSLS the tropospheric transport time
219 scale plays a dominant role for the calculation of their ODP and the concept of a global
220 lifetime τ_X cannot be adapted. Therefore, the global lifetime needs to be replaced by an
221 expression weighting the fraction of VSLS reaching the tropopause and their subsequent
222 residence time in the stratosphere.

223

224 Following a method previously developed specifically for VSLS, the ODP of CHBr₃ is
225 calculated as a function of location and time of emission (x_e, t_e) based on ERA-Interim
226 driven FLEXPART trajectories (Pisso et. al., 2010). Based on the trajectory calculations, the
227 fraction of VSLS reaching the tropopause and the stratospheric residence time are derived.
228 Owing to the different timescales and processes in the troposphere and stratosphere, the
229 estimates are based on separate ensembles of trajectories quantifying the transport in both
230 regions. The tropospheric trajectory ensembles are used to determine the fraction of VSLS
231 reaching the tropopause at different injection points (y, s). The subsequent residence time in
232 the stratosphere is quantified from stratospheric trajectory ensembles run for a longer time
233 period (20 years). ODPs as a function of location and time of emission were obtained from

equation (1) where the expression $\int_{t_e}^{\infty} \int_{\Omega} \sigma r_X^{\Omega} T^{strat} dy ds$ replaces τ_X . This expression integrated in time s starting at the emission time t_e and throughout the surface Ω (representing the tropopause) is estimated from the tropospheric and stratospheric trajectory ensembles. Tropospheric transport appears as the probability $\sigma(y, s; x_e, t_e)$ of injection at (y, s) in Ω while physico-chemical processes in the troposphere appear as the injected proportion of total halogen emitted $r_X^{\Omega}(y, s; x_e, t_e)$. Stratospheric transport is taken into account by $T^{strat}(y, s)$ which expresses the stratospheric residence time of a parcel injected at the tropopause at (y, s) . An ozone depletion efficiency factor of 60 is used for bromine (Sinnhuber et al., 2009). A more detailed derivation of the approximations and parameterizations including a discussion of the errors involved can be found in Pisso et al. (2010).

244

245 **2.3 CHBr₃ mass flux-derived ODP**

246

While present day ODP estimates for VSLS based on ERA-Interim are available (e.g., Pisso et al., 2010), the trajectory-based method has not been applied to future model scenarios so far. Therefore, we attempt to determine an ODP proxy easily available from climate model output, which can be used to derive future estimates of the ODP fields. In general, the ODP of a VSLS as a function of time and location of emission is determined by tropospheric and stratospheric chemistry and transport processes. It has been shown, however, that the effect of spatial variations in the stratospheric residence time on the ODP is relatively weak (Pisso et al., 2010). We identify a pronounced relationship between the ODP of CHBr₃ and deep convective activity, which demonstrates that for such short-lived substances the ODP variability is mostly determined by tropospheric transport processes. Based on the identified relationship we develop a proxy for the ODP of CHBr₃ based on the ERA-Interim convective upward mass flux. For the available trajectory-derived ODP fields, we determine a linear fit [a₀, a₁] with residual r in a least-square sense:

260

$$y = a_0 + a_1 x + r. \quad (2)$$

261

The dependent variable y is the trajectory-based ODP prescribed as a vector of all available monthly mean ODP values comprising 26 months of data re-gridded to the ERA-Interim standard resolution of 1° x 1°. The independent variable x is a vector of the ERA-Interim monthly mean updraught mass flux between 250 and 80 hPa with a 1° x 1° resolution for the same months. The fit coefficients [a₀, a₁] are used to calculate the ODP proxy \hat{y}

267

$$\hat{y} = a_0 + a_1 x. \quad (3)$$

269

The fit scores a coefficient of determination of $r^2 = 0.71$ conveying that our ODP proxy (called mass flux-derived ODP from now on) explains 71% of the variance of the original trajectory-derived ODP fields for the time period 1999-2006. We find good agreement between the trajectory-derived and the mass flux-derived ODP and ODP-weighted CHBr₃ emissions (see Sections 4 and 5 for details). In order to extend the ODP-weighted CHBr₃ emissions beyond 1999 and 2006, we apply the linear fit function $[a_0, a_1]$ to the convective upward mass flux between 250 and 80 hPa from ERA-Interim and from the CESM1-CAM5 runs. Thus we estimate observational (1979-2013), model historical (1979-2005) and model future RCP8.5 (2006-2100) mass flux derived-ODP fields.

279

The ODP of such short-lived substances as CHBr₃ shows a weak dependence on the stratospheric residence time and thus on the latitude of the injection point at the tropopause (Pisso et al., 2010). Our method of deriving the ODP from the convective mass flux neglects the impact of spatial variations in the stratospheric residence time on the ODP. However, within the tropical belt, which is the main region of interest for our analysis with high ODP values and strong convective mass fluxes, the stratospheric residence time can be approximated by a constant as included in the fit coefficients. Similarly, expected future changes of the stratospheric residence time associated with an accelerating stratospheric circulation (Butchart, 2014) are not taken into account in our calculation of the mass flux-derived ODP from model climate predictions. Overall, we expect that tropospheric transport and stratospheric chemistry will have a much larger impact on the future ODP trends than changes in the stratospheric residence time. **We expect that changes in the stratospheric residence time only have small impact on the future ODP, compared to the impacts of tropospheric transport and stratospheric chemistry.** Thus, we do not take the latter into account in our calculation of future ODP-weighted CHBr₃ emissions for the benefit of a cost-efficient computationally-efficient method enabling the estimation of future ODP fields.

296

In addition to changing mass fluxes included in our ODP proxy, changes in stratospheric chemistry will impact the future ODP of CHBr₃. In order to account for less effective catalytic ozone destruction, we apply a changing α -factor to our ODP fields. The bromine α -factor describes the chemical effectiveness of stratospheric bromine ozone depletion relative to chlorine (Daniel et al., 1999) and is set to a global mean value of 60 (Sinnhuber et al., 2009)

for the calculation of 1999–2006 ODP fields (Section 2.2). As most of the bromine induced stratospheric ozone loss is caused by the combined BrO/ClO catalytic cycle, the effect of bromine (and thus the α -factor) is expected to be smaller for decreasing anthropogenic chlorine. We use idealized experiments carried out with the UM-UKCA chemistry–climate model to derive changes in the α -factor of brominated VSLS. The experiments were performed under two different stratospheric chlorine concentrations, corresponding roughly to beginning (3 ppbv Cl_y) and end (0.8 ppbv Cl_y) of the 21st century conditions, and 1xVSLS versus 2xVSLS loading (see Yang et al., 2014 for details). We calculate the difference between the 2xVSLS and 1xVSLS simulations for both chlorine scenarios to get the overall effect of VSLS on ozone for the beginning and end of the 21st century conditions. From the change of this difference from one chlorine scenario to the other, we estimate the global mean α -factor applicable for bromine from VSLS at the end of the century to be around 47. Compared to the current α -factor of 60 this is a reduction of about 22%. For simplicity, we assume the stratospheric chlorine loading from 2000 to 2100 to be roughly linear and estimate the α -factor within this time period based on a linear interpolation between the 2000 and the 2100 value. In a similar manner, we scale the ODP field before 1996 to account for the fact that during this time there was less stratospheric chlorine and a reduced effectiveness of bromine-related ozone depletion. Stratospheric chlorine in 1979 equals roughly the value expected for 2060 (Harris and Wuebbles et al., 2014), thus corresponding to a 13% reduced bromine α -factor of 52. ODP values between 1979 and the year 1996, when the amount of stratospheric chlorine reached a peak and started to level off (Carpenter and Reimann et al., 2014), are estimated based on a linear interpolation over this time period.

324

325 **2.4 ODP-weighted CHBr₃ emissions**

326

327 The concept of ODP-weighted emissions combines information on the emission strength and
328 on the relative ozone-destroying capability of a substance. Its application to VSLS has been
329 recently rendered possible by the availability of observation-based VSLS emission maps
330 (Ziska et al., 2013). Here, we calculate the present-day ODP-weighted emissions of CHBr₃ for
331 data available for four months (March, June, September and December) from 1999 to 2006 by
332 multiplying the CHBr₃ emissions with the trajectory-derived ODP at each grid point. The
333 resulting ODP-weighted emission maps are given as a function of time (monthly averages)
334 and location (1°x1° grid). Global annual means are calculated by averaging over all grid
335 points and over the four given months.

336

337 In order to extend the time series of ODP-weighted CHBr₃ emissions beyond 1999 and 2006,
338 we derive ODP fields from the ERA-Interim upward mass flux. The method is based on the
339 polynomial fit determined for the available trajectory-derived CHBr₃ ODP fields as described
340 in Section 2.3. Multiplying the mass flux-derived ODP fields with the monthly mean emission
341 fields from Ziska et al. (2013) results in a long term time series (1979-2013) of ODP-
342 weighted CHBr₃ emissions. Similarly, we use the CESM1-CAM5 mass flux-derived ODP
343 fields together with emission inventories derived from CESM1-CAM5 meteorological data to
344 produce historical (1979-2005) and future (2006-2100) model-driven ODP-weighted CHBr₃
345 emission fields.

346

347 **3 ODP-weighted CHBr₃ emissions for present day conditions**

348

349 We will introduce the concept of the ODP-weighted emissions of CHBr₃ exemplarily for
350 March 2005 and discuss how the ODP-weighted emissions of this very short-lived compound
351 compare to those of long-lived halogens. The CHBr₃ emissions (Ziska et al., 2013) for March
352 2005 are shown in Figure 1a with highest emissions in coastal regions, in the upwelling
353 equatorial waters and the Northern Hemisphere (NH) mid-latitude Atlantic. The emissions
354 show large variations and reach values higher than 1500 pmol m⁻² hr⁻¹ in coastal regions
355 characterized by high concentrations due to biological productivity and anthropogenic
356 activities. In the tropical open ocean, emissions are often below 100 pmol m⁻² hr⁻¹, while in
357 the subtropical gyre regions, ocean and atmosphere are nearly in equilibrium and fluxes are
358 around zero. Globally, the coastal and shelf regions account for about 80% of all CHBr₃
359 emissions (Ziska et al., 2013). Apart from the gradients between coastal, shelf and open ocean
360 waters the emissions show no pronounced longitudinal variations. Negative emissions occur
361 in parts of the Southern Ocean, northern Pacific and North Atlantic and indicate a CHBr₃ sink
362 given by a flux from the atmosphere into the ocean. The evaluation of various CHBr₃
363 emission inventories from Hossaini et al. (2013) shows that in the tropics the best agreement
364 between model and observations is achieved using the bottom-up emissions from Ziska et al.
365 (2013). In the extratropics, however, the CHBr₃ emissions from Ziska are found to result in
366 too low atmospheric model concentrations diverging from observations by 40 to 60%.

367

368 The potential impact of CHBr₃ on the stratospheric ozone layer is displayed in Figure 1b in
369 form of the ODP of CHBr₃ given as a function of time and location of the emissions but

370 independent of its strength. Overall, the ODP of CHBr₃ is largest in the tropics (tropical ODP
371 belt) and has low values (mostly below 0.1) north and south of 20°. The ODP depends
372 strongly on the efficiency of rapid transport from the ocean surface to the stratosphere which
373 is in turn determined by the intensity of high reaching convection. In the NH winter/spring of
374 most years, the strongest convection and therefore the highest ODP values of up to 0.85 are
375 found over the equatorial West Pacific (Pisso et al., 2010). In contrast to the CHBr₃ emission
376 estimates, the ODP shows pronounced longitudinal variations linked to the distribution of
377 convection and low-level flow patterns.

378

379 The ODP-weighted CHBr₃ emissions for March 2005 are displayed in Figure 2. While the
380 emissions themselves describe the strength of the CHBr₃ sea-to-air flux, the ODP-weighted
381 emissions cannot be interpreted directly as a physical quantity but only relative to ODP-
382 weighted emissions of long-lived halocarbons. The spatial distribution of the ODP-weighted
383 emissions combines information on where large amounts of CHBr₃ are emitted from the
384 ocean and where strong vertical transport enables CHBr₃ to reach the stratosphere. Only for
385 regions where both quantities are large, strong ODP-weighted emissions will be found.
386 Regions where one of the quantities is close to zero will not be important, such as the mid-
387 latitude North Atlantic where large CHBr₃ emissions occur but the ODP is very low. Negative
388 ODP-weighted emissions occur in regions where the flux is from the atmosphere into the
389 ocean. Since negative ODP-weighted emissions are not a meaningful quantity and occur in
390 regions where the ODP is small they will not be displayed in the following figures and are not
391 taken into account for the calculations of the global mean values. The ODP-weighted
392 emissions are in general largest between 20°S and 20°N (72% of the overall global amount)
393 as a result of the tropical ODP belt and peak at the equator and tropical coast lines as a result
394 of the emission distribution. The distribution of the ODP-weighted emissions demonstrates
395 clearly that CHBr₃ emissions from the NH and Southern Hemisphere (SH) extratropics have
396 negligible impact on stratospheric ozone chemistry. Thus, the fact that the emissions from
397 Ziska et al. (2013) might be too low in the extratropics (Hossaini et al., 2013) does not impact
398 our results. Of particular importance for the stratosphere, on the other hand, are emissions
399 from the Maritime Continent (South-East Asia), the tropical Pacific and the Indian Ocean.

400

401 The global annual mean ODP-weighted emissions of CHBr₃ are about 40 Gg/year for 2005
402 (Figure 3) based on the March, June, September and December values of this year. The
403 concept of ODP-weighted emissions becomes particularly useful when comparing this

404 quantity for CHBr₃ with the ones of manmade halocarbons. For the year 2005, ODP-weighted
405 emissions of CHBr₃ amount up to 50% of the ODP-weighted emissions of methyl bromide
406 (CH₃Br, natural and anthropogenic), of CFC-11, or of CFC-12 (CCl₂F₂) and are of similar
407 magnitude as the ODP-weighted emissions of CCl₄ and the individual halons. While the ODP
408 of CHBr₃ exceeds the value of 0.5 only in less than 10% **of the regions** over the globe, the
409 relatively large CHBr₃ emissions make up for the overall relatively small ODPs. Current
410 estimates of global CHBr₃ emissions range between 249 Gg/year and 864 Gg/year (Ziska et
411 al., 2013 and references therein), with the higher global emission estimates coming from top-
412 down methods while the lower boundary is given by the bottom-up study from Ziska et al.
413 (~~Already this lower boundary of the unweighted CHBr₃ emissions exceeds the combined~~
414 ~~emissions of the most abundant CFCs.~~ For our study, even the choice of the lowest emission
415 inventory leads to relatively large ODP-weighted emissions of the very short-lived CHBr₃ as
416 discussed above. Choosing a different emission inventory than Ziska et al. (2013) would
417 result in ~~even~~ larger ODP-weighted CHBr₃ emissions. Still more important than the overall
418 CHBr₃ emission strength is the fact that emissions and ODP show **similar** ~~the same~~ latitudinal
419 gradients with both fields having higher values at the low latitudes. This spatial coincidence
420 of large sources and efficient transport **leads to** ~~causes~~ the relatively large global mean value
421 of ODP-weighted CHBr₃ emissions.

422
423 It is important to keep in mind that the long-lived halocarbons are to a large degree of
424 anthropogenic origin, while CHBr₃ is believed to have mostly natural sources. However,
425 CHBr₃ in coastal regions also results from anthropogenic activities such as aqua-farming in
426 South-East Asia (Leedham et al., 2013) and oxidative water treatment (Quack and Wallace,
427 2003). While these sources accounted for only a small fraction of the global budget in 2003
428 (Quack and Wallace, 2003), their impact is increasing. In particular, aqua-farming used,
429 among other things, for food production and CO₂ sequestering has started to increase as an
430 anthropogenic VSL source. Leedham et al. (2013) estimated tropical halocarbon production
431 from macroalgae in the Malaysian costal region and suggest that only 2% of the local CHBr₃
432 emissions originate from farmed seaweeds. However, based on recent production growth
433 rates, the Malaysian seaweed aquaculture has been projected to experience a 6-11 fold
434 increase over the next years (Phang et al., 2010). More importantly, other countries such as
435 Indonesia, Philippines and China are known to produce considerably more farmed seaweed
436 than Malaysia (e.g., Tang et al., 2011), but their contribution to the total anthropogenic VSL
437 emissions has not yet been assessed. The ODP of CHBr₃ demonstrates the high sensitivity of

438 the South-East Asia region to growing emissions. Globally the highest ODP values (Figure
439 1b) are found in the same region where we expect future anthropogenic CHBr₃ emissions to
440 increase substantially. An assessment of current and future seaweed farming activities
441 including information on farmed species, fresh or dry weight macro algal biomass and
442 incubation derived halocarbon production values is required to estimates the net oceanic
443 aquaculture VSLS production. Since the general ODP concept has been originally defined for
444 anthropogenic halogens, the ODP-weighted CHBr₃ emissions should be calculated for the
445 anthropogenic component of the emissions. However, since no such estimates are available at
446 the moment, the method is applied to the combined emission field. Given that the natural
447 oceanic production and emissions of halogenated VSLS are expected to change in the future
448 due to increasing ocean acidification, changing primary production and ocean surface
449 meteorology (Hepach et al., 2014), it will remain a huge challenge to properly separate natural
450 and anthropogenic emissions of these gases.

451

452

453 **4 ODP proxy**

454

455 It is necessary to understand the short and long-term changes of the ODP-weighted CHBr₃
456 emissions in order to predict their future development. On the seasonal time scales, the ODP-
457 weighted CHBr₃ emissions show large variations as demonstrated in Figure 4 for June and
458 December 2001. In the NH summer, 57% of the ODP-weighted emissions stem from the NH
459 tropical belt (30°N-0°N) with largest contributions from the Maritime Continent and Asian
460 coastal areas. In the NH winter, the ODP-weighted emissions shift to the SH tropical belt
461 (48%) with **the** strongest contributions from the West Pacific. While the Maritime Continent
462 is an important source region all-year around, emissions from the southern coast line of Asia
463 during NH winter are not very important for stratospheric ozone depletion. The emissions
464 reveal some seasonal variations **which are most apparent in the Indian Ocean with peak**
465 **values during NH summer along the equator and along the NH coast lines (see Fig. S1 in**
466 **the Supplement). Note that CHBr₃ concentrations maps represent climatological fields**
467 **and the seasonal variations in the emission fields stem from varying surface winds and sea**
468 **surface temperature (see Section 2.1). Global average CHBr₃ emissions show a seasonal**
469 **cycle of about 25% with a maximum in July and a minimum in April (Ziska et al., 2013).**

470 The seasonality of the ODP (Figure 5a) **driven by the seasonality of deep convection**

471 **amplifies the seasonal variations in the emissions and thus** causes the pronounced shift of
472 the ODP-weighted emissions from one hemisphere to the other.

473

474 We want **In oder to** analyze the long-term changes of ODP-weighted CHBr₃ emissions, we
475 need to extend the time series beyond the 1999-2006 **time period**. While CHBr₃ emissions
476 are available for 1979-2013, the ODP itself, based on costly trajectory calculations, is
477 restricted to 1999-2006. In order to develop an ODP proxy, we first analyze the variations of
478 the trajectory-derived ODP fields and their relation to meteorological parameters. The ODP
479 fields for the months June and December 2001 shown in Figure 5a have their maxima
480 between 0°N and 20°N for the NH summer and 5°N and 15°S for the NH winter. In the NH
481 summer, the dominant source region for stratospheric CHBr₃ is located in the equatorial West
482 Pacific region including **Southeast** Asia. In the NH winter, the source region is shifted
483 westward and southward with its center now over the West Pacific. These seasonal variations
484 agree with results from previous trajectory studies (e.g., Fueglistaler et al., 2005; Krüger et al.,
485 2008) and are consistent with the main patterns of tropical convection (Gettelman et al.,
486 2002).

487

488 A detailed picture of the high reaching convective activities for June and December is given
489 in Figure 5b in form of the ERA-Interim monthly mean updraught mass flux between 250 and
490 80 hPa. The rapid updraughts transporting air masses from the boundary layer into the tropical
491 tropopause layer (TTL) are part of the ascending branch of the tropospheric circulation
492 constituted by the position of the intertropical convergence zone (ITCZ). The updraught
493 convective mass fluxes are largest in and near the summer monsoon driven circulations close
494 to the equator. Over the West Pacific and Maritime Continent the region of intense convection
495 is quite broad compared to the other ocean basins due to the large oceanic warm pool and
496 strong monsoon flow. In addition to the overall annual north-south migration pattern, large
497 seasonal changes of the updraught mass flux are visible over South America and the Maritime
498 Continent consistent with the climatological distribution of the ITCZ. The **southeastward**
499 pointing extension in the Pacific is strongest in the NH winter and indicates a double ITCZ.
500

501 We derive a CHBr₃ ODP proxy from the ERA-Interim updraught mass fluxes (referred to as
502 mass flux-derived ODP, see Section 2.3 for details). While the downdraught mass fluxes can
503 also impact (5-15%) the composition in the upper troposphere/lower stratosphere (Frey et al.,
504 2015), they are not included in our proxy since their importance for the contribution of CHBr₃

505 to stratospheric bromine is less clear and cannot be prescribed by a fit relation. The strong
506 correlation between CHBr₃ ODP and high-reaching convection justifies our method by
507 indicating that we capture the most important process for explaining the ODP variability. The
508 mass flux-derived ODP fields are shown in Figure 5c and explain 76% and 81% of the
509 variance of the original trajectory-derived ODP fields (Figure 5a). Differences between the
510 trajectory-derived ODP fields and the mass flux-derived proxy may be caused by the fact that
511 not only the location of the most active convective region will determine the ODP distribution
512 but also patterns of low-level flow into these regions. Additionally, spatial and seasonal
513 variations in the expected stratospheric residence time may have a small impact on the
514 trajectory-derived ODP and cause deviations to the mass flux-derived proxy. Largest
515 disagreement between the trajectory-derived and mass flux-derived ODP is found over South
516 America and Africa. However, the ODP values over the continents are not important for the
517 ODP-weighted CHBr₃ emissions due to the very low to non-existent emissions over land
518 (Quack and Wallace, 2003) and are not used in our study.

519
520 Our analysis confirms that the ODP of species with short lifetimes, such as CHBr₃, is to a
521 large degree determined by the high-reaching convective activity (Pisso et al., 2010). As a
522 result, updraught mass flux fields can be used to derive a proxy of the ODP fields. Such a
523 proxy can also be derived from related meteorological parameters such as the ERA-Interim
524 detrainment rates (not shown here). The ODP proxies identified here provide a cost-efficient
525 method to calculate ODP fields for past (ERA-Interim) and future (climate model output)
526 meteorological conditions. Long-term changes in stratospheric chemistry due to declining
527 chlorine background levels are taken into account by variations of the bromine α -factor (see
528 Section 2.3 for details). Our method enables us to analyze long-term changes of the ODP and
529 the ODP-weighted emissions, which would otherwise require very large computational
530 efforts.

531
532 **5 ODP-weighted CHBr₃ emissions for 1979-2013**

533
534 Based on the ODP proxy and the correction of the α -factor introduced in Section 4, we
535 calculate ODP-weighted CHB₃ emission fields for the ERA-Interim time period from 1979 to
536 2013. As a test for our method, we compare the global mean ODP-weighted emissions based
537 on the trajectory- and mass flux-derived ODP fields for the years 1999-2006. The two time
538 series of ODP-weighted emissions are displayed in Figure 6 and show a very good agreement

539 with slightly lower mass flux-derived values (green line) than trajectory-derived values (black
540 line). Individual months can show stronger deviations, e.g., for December 1999 the mass flux-
541 derived ODP-weighted emissions are about 30% smaller than the trajectory-derived ones. The
542 pronounced seasonal cycle with maximum values in the NH summer and autumn is captured
543 by both methods. The seasonal cycle of the global mean values is mostly caused by the very-
544 high ODP-weighted emissions along the South-East Asian coast line which are present during
545 the NH summer/autumn, but not during the NH winter. **The same signal is evident from the**
546 **CHBr₃ emissions itself (see Figure S1 in the Supplement) and is amplified by the shift of**
547 **high ODP values to the NH tropics during NH summer (Figure 5a and c). The**
548 **pronounced seasonal cycle of the ODP-weighted emissions indicates a seasonality of the**
549 **CHBr₃ concentrations in the TTL, which needs to be verified by observations.** Note that
550 the ODP-weighted emissions of long-lived halocarbons discussed in Section 3 show no strong
551 seasonal variations. The good agreement between the trajectory-derived and the mass flux-
552 derived ODP-weighted CHBr₃ emissions encourages the use of the latter for the analysis of
553 longer time series.

554

555 The 35-year long time series (1979-2013) of ODP-weighted CHBr₃ emissions is based on the
556 ERA-Interim surface parameters, TTL convective mass flux and a changing bromine α -factor
557 (Figure 7a). The time series is relatively flat over the first 27 years ranging from 34 Gg/year
558 to 39 Gg/year. Over the last years from 2006 to 2013, a steep increase occurred and ODP-
559 weighted CHBr₃ emissions of more than 41 Gg/year are reached. In order to analyze which
560 component, the mass flux-derived ODP fields, the oceanic emissions or the stratospheric
561 chemistry, causes this steep increase, three sensitivity studies are performed. In the first study,
562 the emissions vary over the whole time period (1979-2013), while the ODP field and the
563 bromine α -factor are held fixed at their 35-year mean values. Changes in the resulting, global
564 mean ODP-weighted emission time series (Figure 7b) are driven by changes in the emissions
565 alone and show a steady increase over the whole time period of about 2.2% per decade. This
566 is in agreement with the linear trend of the global mean CHBr₃ emissions estimated to be
567 7.9% over the whole time period caused by increasing surface winds and sea surface
568 temperatures (Ziska et al., in prep). We do not necessarily expect the two trends to be
569 identical, since the ODP-weighted emissions only include emissions in convective active
570 regions, while the global mean emissions correspond to non-weighted mean values including
571 CHBr₃ emissions from middle and high latitudes.

572

573 For the second study, the emission fields and the α -factor are kept constant at the 35-year
574 mean values and the mass flux-derived ODP is allowed to vary with time. Changes in the
575 resulting, global mean ODP-weighted emission time series (Figure 7c) are mainly driven by
576 changes in the tropical high-reaching convection and show a negative trend from 1979 to
577 2005 of -3.4% per decade. Over the years 2006-2013, however, changes in convective activity
578 lead to a steep increase of the ODP-weighted emissions. These changes can either result from
579 a general strengthening of the tropical convective activity or from changing patterns of
580 convective activity, shifting regions of high activity so that they coincide with regions of
581 strong CHBr₃ emissions. For the third sensitivity study, the emissions and mass flux-derived
582 ODP are kept constant at the 35-year mean values, while the α -factor varies with time
583 according to the stratospheric chlorine loading. ODP-weighted CHBr₃ emissions increase by
584 13% from 1979 to 1999 and peak during the time of the highest stratospheric chlorine loading
585 from 1999 to 2006. Overall, variations of the ODP-weighted CHBr₃ emissions induced by the
586 stratospheric chlorine-related chemistry are in the same range as the variations induced by
587 changes in convective transport and oceanic emissions.

588

589 Combining the conclusions of all three sensitivity studies reveals that for the time period 1979
590 to 2005, the positive trend of the emissions and the α -factor on the one hand and the negative
591 trend of the mass flux-derived ODP on the other hand mostly cancel out leading to a flat time
592 series of ODP-weighted CHBr₃ emissions (Figure 7a) with no long-term changes. From 2005
593 to 2013, however, a strong increase in ODP and continuously increasing emissions lead to a
594 step-like increase of the ODP-weighted CHBr₃ emissions from 35 Gg/year to 41 Gg/year.

595

596 **6 Model-derived ODP-weighted CHBr₃ emissions**

597

598 We aim to estimate ODP-weighted CHBr₃ emissions from earth system model runs.
599 Therefore, we use CHBr₃ emissions and the CHBr₃ ODP proxy calculated with CESM1-
600 CAM5 sea surface temperature, surface wind and upward mass flux, respectively (see Section
601 2 for details). In a first step, we evaluate how well the results of our analysis based on the
602 earth system model compare to the results based on ERA-Interim. Figure 8a shows the
603 distribution of the three quantities, CHBr₃ emissions, mass flux-derived ODP and ODP-
604 weighted emissions, for ERA-Interim and CESM1-CAM5 exemplary for March 2000. The
605 distribution of the emission field is very similar between ERA-Interim and CESM1-CAM5.
606 Largest deviations are found in the Indian Ocean along the equator, where higher surface

607 winds and temperatures in the model force a stronger sea-to-air flux. Note that in this region,
608 very limited observational data was available for the construction of the emission inventories
609 and future updates will reveal, if these isolated data points are representative for the equatorial
610 Indian Ocean.

611

612 The ERA-Interim mass flux-derived CHBr₃ ODP (Figure 8b) shows an almost zonally
613 uniform region of higher ODP values (around 0.4) extending south of the equator down to
614 20°S. In contrast, the CESM1-CAM5 mass flux-derived ODP shows only three regions in the
615 ~~inner deep~~ tropics (the Maritime continent, Africa, South America) with values exceeding
616 0.3. While the ODP from CESM1-CAM5 ~~show higher local maxima can reach locally~~
617 ~~higher values~~ than the ODP from ERA-Interim, the globally averaged ODP field is larger for
618 the reanalysis data than for the model. As a result, the ODP-weighted CHBr₃ emissions
619 (Figure 8c) based on reanalysis data are higher in most of the tropics. Particularly, in the East
620 Pacific and Indian Ocean large scale features of enhanced ODP-weighted CHBr₃ emissions
621 exist for ERA-Interim but not for the earth system model. On the other hand, enhanced ODP-
622 weighted emissions along some coast lines are present in the model results (e.g., Indonesia)
623 but are not as pronounced in ERA-Interim. Overall, the ODP-weighted CHBr₃ emissions for
624 March 2000 based on ERA-Interim and CESM1-CAM5 show similar distribution and similar
625 magnitude. The model-derived values are slightly smaller than the observation-derived values
626 mostly as a result of less high-reaching convective activity in the model.

627

628 We compare the global mean ODP-weighted CHBr₃ emissions based on the ERA-Interim
629 reanalysis data (observation-derived) to the same quantity from the CESM1-CAM5 historical
630 model run for the 1999-2006 time period (Figure 9). The historical ODP-weighted emissions
631 from CESM1-CAM5 show larger variations than the observation-derived time series. The
632 stronger variability is caused by a stronger variability in the ODP time series possibly related
633 to larger meteorological fluctuations in the earth system model during this short time period.
634 The overall magnitude as well as the phase and amplitude of the seasonal cycle are ~~captured~~
635 reasonably well ~~captured~~ by CESM1-CAM5, ~~encouraging lending confidence in~~ the use of
636 the model to estimate ODP-weighted CHBr₃ emissions for future climate scenarios. Recent
637 improvements have been reported in the regional cloud representation in the deep convective
638 tropical Pacific (Kay et al., 2012) and in the parameterization of deep convection and ENSO
639 simulation (Neale et al., 2008). Overall, our analysis demonstrates that the spatial and

640 seasonal variability of the model fields allows to derive realistic ODP-weighted CHBr₃
641 emission estimates.

642

643 **7 ODP-weighted CHBr₃ emissions for 2006-2100**

644

645 Future ODP-weighted CHBr₃ emissions shown in Figure 10a are based on future model
646 estimates of the CHBr₃ emissions and the CHBr₃ ODP proxy. Both quantities are calculated
647 based on the meteorological and marine surface variables and convective mass flux from the
648 CESM1-CAM5, RCP8.5 runs. In addition, we have applied a correction factor to the ODP
649 fields to account for a changing α -factor based on less effective ozone loss cycles in the
650 stratosphere due to the decrease of anthropogenic chlorine (Section 2.3). The future estimates
651 of the ODP-weighted CHBr₃ emissions show pronounced interannual variations of up to 20%.
652 Overall, the ODP-weighted emissions increase steadily until 2100 by about 31% of the 2006-
653 2015 mean value corresponding to a linear trend of 2.6% per decade.

654

655 In order to analyze what causes the strong interannual variability and the long-term trend, we
656 conduct sensitivity studies where only one factor (emissions, mass flux-derived ODP,
657 stratospheric chemistry) is changing while the other two are kept constant. Figure 10b
658 displays the time series of ODP-weighted CHBr₃ emissions for varying oceanic emission
659 fields. The emission-driven time series for 2006-2100 shows a positive trend of 2.2% per
660 decade which is in the range of the trend observed for the emission-driven time series for
661 1979-2013 based on ERA-Interim (Figure 7b). However, the model-based ODP-weighted
662 emissions show no long-term change over the first 15 years and the positive, emission-driven
663 trend only starts after 2020. The second sensitivity study (Figure 10c) highlights changes in
664 the ODP-weighted emissions attributable to high-reaching convection (via the mass flux-
665 derived ODP), while emission fields and α -factor are kept constant. Clearly, the strong
666 interannual variations in the combined time series (Figure 10a) are caused by the same
667 fluctuations in the mass flux-driven time series. In comparison, the interannual variability of
668 the emission-driven time series is less pronounced. The projected changes in atmospheric
669 transport cause a positive trend of the ODP-weighted emissions of about 3.1% per decade.
670 This positive trend projection in the mass flux-derived ODP reveals a future change in the
671 tropical circulation with significant consequences for trace gas transport from the troposphere
672 into the stratosphere. More detailed evaluations demonstrate that the CESM1-CAM5 tropical
673 convective upward mass flux is projected to decrease in the lower and middle troposphere

674 (not shown here) in agreement with results from UKCA chemistry-climate model simulations
675 (Hossaini et al., 2012). Contrary to the changes in the middle troposphere, the convective
676 mass flux in the upper troposphere (above the 250 hPa level), is projected to increase in the
677 future again in agreement with Hossaini et al. (2012). A higher extension of tropical deep
678 convection has also been found in other model projections and ~~global warming~~ **increased**
679 **greenhouse gas induced tropospheric warming** leading to an uplift of the tropopause has
680 been suggested as the possible cause (Chou and Chen, 2010; Rybka and Tost, 2014). Overall,
681 an increasing upward mass flux in the upper troposphere/lower stratosphere would lead to
682 enhanced entrainment of CHBr₃ into the stratosphere, consistent with results from Hossaini et
683 al. (2012) and Dessens et al. (2009), and thus to increasing ODP-weighted emissions. Finally,
684 for the last sensitivity study, the chemistry-driven time series of the ODP-weighted emissions
685 shows no interannual variability and a negative trend of -2.6% per decade. Decreasing
686 anthropogenic chlorine emissions and thus a less efficient BrO/ClO ozone loss cycle lead to a
687 reduction of bromine-related ozone depletion of 22% as prescribed by the results of the
688 idealized chemistry-climate model experiments from Yang et al. (2014).

689

690 In summary, changing emissions and changing convection lead to a projected increase **of**
691 **5.4% per decade** of the ODP-weighted emissions over the 21st century **for the RCP8.5**
692 **scenario**. ~~If only these two factors would impact the ODP weighted emissions, a positive~~
693 ~~trend of 5.4% per decade would be expected based on RCP8.5 model simulations.~~ However,
694 due to declining anthropogenic chlorine, stratospheric ozone chemistry will become less
695 effective and the corresponding decreasing α -factor reduces the ODP-weighted CHBr₃
696 emissions resulting in an overall projected trend of about 2.6% per decade.

697

698 A comparison of the model-derived CHBr₃ ODP-weighted emissions with the ones of other
699 long-lived substances is shown in Figure 11. For the other ozone depleting substances
700 included in the comparison, changing emissions are taken into account by applying their
701 potential emission scenarios (Velders et al., 2007; Ravishankara et al., 2009). The ODP of
702 CFC-11 is nearly independent of the stratospheric chlorine levels (Ravishankara et al.,
703 2009), and is thus kept constant for the whole time period. The same is assumed for all other
704 long-lived halocarbons included in the comparison. Our comparison shows that emissions of
705 the short-lived CHBr₃ can be expected to have a larger impact on stratospheric ozone than the
706 other anthropogenic halocarbons after approximately 2025 (Figure 11). Two exceptions to

707 this are ODP-weighted emissions of CH₃Br and anthropogenic N₂O (Ravishankara et al.,
708 2009) both not shown in our plot.

709

710 CH₃Br, with partially anthropogenic and partially natural sources, is not included in the
711 comparison, since no potential emission scenario and no estimate on how changes in
712 atmospheric transport will impact its ODP are available at the moment. If we would assume a
713 CH₃Br scenario with constant emissions from natural and anthropogenic sources and a
714 constant α -factor, its ODP weighted emissions would be around 70 Gg/year over the 21st
715 century. However, we know this to be unrealistic and expect changes in anthropogenic CH₃Br
716 emissions and a decreasing α -factor which would both lead to smaller projections of its ODP-
717 weighted emissions. N₂O emissions have been projected to be the most important ozone-
718 depleting emissions in the future with ODP-weighted emissions between 100 and 300 Gg/year
719 expected for the end of the century (Ravishankara et al., 2009).

720

721 **8 Discussion and summary**

722

723 The ODP-weighted emissions of CHBr₃ give a detailed picture on where and when oceanic
724 CHBr₃ emissions take place that will later impact stratospheric ozone. Furthermore, they
725 provide a useful tool of comparing the emission strength of CHBr₃ with the ones of long-lived
726 anthropogenic gases in an ozone depletion framework. Since currently no information is
727 available on the strength of anthropogenic CHBr₃ emissions, the ODP concept is applied to
728 the complete emission budget including the natural oceanic contribution. While we focus our
729 analysis on one VSLS and introduce the method and application within a case-study
730 framework for CHBr₃, the concept can be applied to all VSLS where emissions and ODP are
731 available at a spatial resolution necessary to describe their variability.

732

733 While the ODP-weighted emissions are an important step towards assessing the current and
734 future effects of VSLS on the ozone layer, one needs to keep in mind that the absolute values
735 are subject of large uncertainties arising from uncertainties in the emission inventories and in
736 the parameterization of the convective transport. Existing global CHBr₃ emission inventories
737 show large discrepancies due to sparse observational data sets and a particularly high
738 uncertainty in coastal emissions ~~from~~ **due to** differing types and amounts of macroalgae
739 (Carpenter and Reimann et al., 2014). We have used the Ziska et al. (2013) emission
740 inventory which suggests a lower flux of CHBr₃ from the tropical oceans to the atmosphere

741 than the other inventories. Based on comparison of the emission inventories in Hossaini et al.
742 (2013) we would expect that the application of a different emission scenario in our approach
743 could lead to ~~two to three times higher~~ **a two to three-fold increase in** ODP-weighted
744 emissions. However, for the tropics, the relatively low emissions from Ziska et al. (2013)
745 provide the best fit with the limited available atmospheric data (Hossaini et al., 2013). The
746 sensitivity of our results to uncertainties in transport becomes apparent when we apply the
747 ODP fields calculated from FLEXPART trajectories without taking into account convective
748 parameterization (Pisso et al., 2010). The ODP calculated without convective
749 parameterization results in roughly 50% lower global mean ODP-weighted CHBr₃ emissions.
750 Additionally, uncertainties may arise from the simplified tropospheric and stratospheric
751 chemistry schemes with an altitude-independent α -factor and a prescribed tropospheric
752 lifetime. Further detailed studies including different convective parameterization schemes,
753 more detailed representation of tropospheric chemistry, product gas impacts, various emission
754 inventories and multi-model mean scenarios are required in order to obtain reliable
755 uncertainty ranges which need to be included in any communication of ODPs to policy
756 makers.

757

758 Our analysis reveals that the spatial variability of trajectory-derived ODP fields of species
759 with short lifetimes, such as CHBr₃, is to a large degree determined by deep tropical
760 convection. As a result, a cost-efficient method to calculate ODP field proxies from updraught
761 mass flux fields has been developed and applied. Past ODP-weighted CHBr₃ emission
762 estimates have been derived based on ERA-Interim meteorological fields. For the time period
763 1979 to 2005, a positive trend in the CHBr₃ emissions and a negative trend in mass flux-
764 derived ODP mostly cancel out leading to a flat time series of ODP-weighted emissions with
765 no long-term changes. From 2006 to 2013, however, a strong increase in both quantities leads
766 to a step-like increase of the ODP-weighted CHBr₃ emissions.

767

768 Future ODP-weighted CHBr₃ emission estimates have been derived from CESM1-CAM5
769 RCP8.5 runs taking into account changing meteorological and marine surface parameters,
770 convective activity and stratospheric chemistry. Changes in tropospheric chemistry and
771 stratospheric residence time are not taken into account for the calculation of the future ODP-
772 weighted emissions. While our methodology is somewhat limited by these simplifications,
773 CHBr₃ delivery from the surface to the tropopause in a future changing climate is expected to
774 be mostly related to changes in tropospheric transport rather than changes in tropospheric

775 chemistry (Hossaini et al., 2013) suggesting that we include the most important processes
776 here. Furthermore, we do not account for changing biogeochemistry in the ocean and
777 anthropogenic activities that can lead to increasing CHBr₃ emissions and further amplify the
778 importance of VSLS for stratospheric ozone chemistry. Such changes in the oceanic sources
779 are important for estimating the future impact of VSLS on atmospheric processes, but are not
780 understood well enough yet to derive reliable future projections. Finally, we do not consider
781 potential future changes in stratospheric aerosol which could impact the contribution of VSLS
782 to stratospheric ozone depletion (Salawitch et al., 2005; Sinnhuber et al., 2006). Variations in
783 the background stratospheric aerosol loading (e.g., Vernier et al., 2011) are mostly attributed
784 to minor volcanic eruptions (Neely et al., 2013). Since future volcanic eruptions are not
785 accounted for in the simulations scenarios used here, we do not include the impact of natural
786 aerosol variations. Suggested future geo-engineering would intentionally enhance the
787 stratospheric aerosol loading and is projected to increase the impact of VSLS on stratospheric
788 ozone by as much as 2% at high latitudes (Tilmes et al., 2012). Such a scenario is not included
789 in our simulations, but could effectively enhance the ODP of CHBr₃ due to an enhanced
790 BrO/ClO ozone loss cycle in the lower stratosphere (Tilmes et al., 2012). Overall, some
791 discrepancies between the observation- and model-derived ODP-weighted CHBr₃ emissions
792 exist, very likely related to out of phase tropical meteorology in the model. However, there is
793 general good agreement between the spatial and seasonal variability of the observation- and
794 model-derived fields, giving us confidence to use this model to derive realistic ODP-weighted
795 CHBr₃ emission estimates.

796
797 Variability of the ODP-weighted CHBr₃ emissions on different time scales are driven by
798 different processes. Spatial and seasonal variations are caused by variations in the surface to
799 tropopause transport via deep convection. Inter-annual variability is mostly driven by
800 transport but also by the variability in the oceanic emissions. Both processes are weakly
801 correlated on inter-annual time scales (with a Pearson correlation coefficient between the
802 interannual anomalies of $r=0.3$), suggesting that in years with stronger emissions (driven by
803 stronger surface winds and higher temperatures) stronger troposphere-to-stratosphere
804 transport exist. The long-term trend, finally, can be attributed in equal parts to changes in
805 emissions, troposphere-**to-stratosphere** transport and stratospheric chemistry. While growing
806 oceanic emissions and changing convective activity lead to increasing ODP-weighted CHBr₃
807 emissions, the expected decline in stratospheric chlorine background levels has the opposite
808 effect and leads to a decrease. Taking all three processes into account, the future model

809 projections suggest a 31% increase of the 2006 ODP-weighted CHBr₃ emissions until 2100
810 for the RCP8.5 scenario. This anthropogenically driven increase will further enhance the
811 importance of CHBr₃ for stratospheric ozone chemistry.

812

813 **Acknowledgements** The authors are grateful to the ECMWF for making the reanalysis
814 product ERA-Interim available. This study was carried out within the EU project SHIVA
815 (FP7-ENV-2007-1-226224) and the BMBF project ROMIC THREAT (01LG1217A). We
816 thank Steve Montzka for helpful discussions.

817 **References**

- 818
- 819 Aschmann, J. and Sinnhuber, B.-M.: Contribution of very short-lived substances to
820 stratospheric bromine loading: uncertainties and constraints, *Atmos. Chem. Phys.*, 13, 1203-
821 1219, doi:10.5194/acp-13-1203-2013, 2013.
- 822
- 823 Austin, J., N., and Butchart, N.: Coupled chemistry-climate model simulations for the period
824 1980 to 2020: ozone depletion and the start of ozone recovery, *Quarterly Journal of the Royal*
825 *Meteorological Society*, 129: 3225–3249, 2006.
- 826
- 827 Braesicke, P., Keeble, J., Yang, X., Stiller, G., Kellmann, S., Abraham, N. L., Archibald, A.,
828 Telford, P., and Pyle, J. A.: Circulation anomalies in the Southern Hemisphere and ozone
829 changes, *Atmos. Chem. Phys.*, 13, 10677– 10688, doi:10.5194/acp-13-10677-2013, 2013.
- 830
- 831 Brioude, J., R. W. Portmann, J. S. Daniel, O. R. Cooper, G. J. Frost, K. H. Rosenlof, C.
832 Granier, A. R. Ravishankara, S. A. Montzka, and A. Stohl: Variations in ozone depletion
833 potentials of very short-lived substances with season and emission region. *Geophys. Res.*
834 *Lett.*, 37, L19804, doi:10.1029/2010GL044856, 2010.
- 835
- 836 Butchart, N.: The Brewer-Dobson circulation, *Rev. Geophys.*, 52,
837 doi:10.1002/2013RG000448, 2014.
- 838
- 839 L.J. Carpenter and S. Reimann (Lead Authors), J.B. Burkholder, C. Clerbaux, B.D. Hall, R.
840 Hossaini, J.C. Laube, and S.A. Yvon-Lewis, Ozone-Depleting Substances (ODSs) and Other
841 Gases of Interest to the Montreal Protocol, Chapter 1 in *Scientific Assessment of Ozone*
842 *Depletion: 2014*, Global Ozone Research and Monitoring Project—Report No. 55, World
843 Meteorological Organization, Geneva, Switzerland, 2014.
- 844
- 845 Chou, C. and Chen, C.: Depth of Convection and the Weakening of Tropical Circulation in
846 Global Warming. *J. Climate*, 23, 3019–3030, doi: doi:10.1175/2010JCLI3383.1, 2010.
- 847
- 848 Daniel, J. S., Solomon, S., Portmann, R. W., and Garcia, R. R.: Stratospheric ozone
849 destruction: The importance of bromine relative to chlorine, *J. Geophys. Res.*, 104, 23871–
850 23880, 1999.

- 851
- 852 Dee, D. P., et al.: The ERA-Interim reanalysis: configuration and performance of the data
853 assimilation system, *Quarterly Journal of the Royal Meteorological Society*, 137(656), 553–
854 597, doi:10.1002/qj.828, 2011.
- 855
- 856 Dessens, O., Zeng, G., Warwick, N. and Pyle, J.: Short-lived bromine compounds in the lower
857 stratosphere; impact of climate change on ozone, *Atmos. Sci. Lett.*, 10(3), 201–206, 2009.
- 858
- 859 Dorf, M., J.H. Butler, A. Butz, C. Camy-Peyret, M.P. Chipperfield, L. Kritten, S.A. Montzka,
860 B. Simmes, F. Weidner, and K. Pfeilsticker: Long-term observations of stratospheric bromine
861 reveal slow down in growth, *Geophys. Res. Lett.*, 33, L24803, doi: 10.1029/2006GL027714,
862 2006.
- 863
- 864 Frey, W., R. Schofield, P. Hoor, D. Kunkel, F. Ravagnani, A. Ulanovsky, S. Viciani, F.
865 D'Amato, and T. P. Lane, The impact of overshooting deep convection on local transport and
866 mixing in the tropical upper troposphere/lower stratosphere (UTLS), *Atmospheric Chemistry*
867 and Physics, 15(11), 6467–6486, doi:10.5194/acp-15-6467-2015, 2015.
- 868
- 869 Fueglistaler, S., M. Bonazzola, P. H. Haynes, and T. Peter: Stratospheric water vapor
870 predicted from the Lagrangian temperature history of air entering the stratosphere in the
871 tropics, *J. Geophys. Res.*, 110, D08107, doi:10.1029/2004JD005516, 2005.
- 872
- 873 Gettelman, A., M. L. Salby, and F. Sassi, Distribution and influence of convection in the
874 tropical tropopause region, *J. Geophys. Res.*, 107(D10), doi:10.1029/2001JD001048, 2002.
- 875
- 876 N. R. P. Harris and D. J. Wuebbles (Lead Authors), J.S. Daniel, J. Hu, L.J.M. Kuijpers, K.S.
877 Law, M. J. Prather, R. Schofield, Scenarios and Information for Policymakers, Chapter 5 in
878 Scientific Assessment of Ozone Depletion: 2014, Global Ozone Research and Monitoring
879 Project—Report No. 55, World Meteorological Organization, Geneva, Switzerland, 2014.
- 880
- 881 Hepach, H., Quack, B., Ziska, F., Fuhlbrügge, S., Atlas, E. L., Krüger, K., Peeken, I., and
882 Wallace, D. W. R.: Drivers of diel and regional variations of halocarbon emissions from the
883 tropical North East Atlantic, *Atmos. Chem. Phys.*, 14, 1255-1275, doi:10.5194/acp-14-1255-
884 2014, 2014.

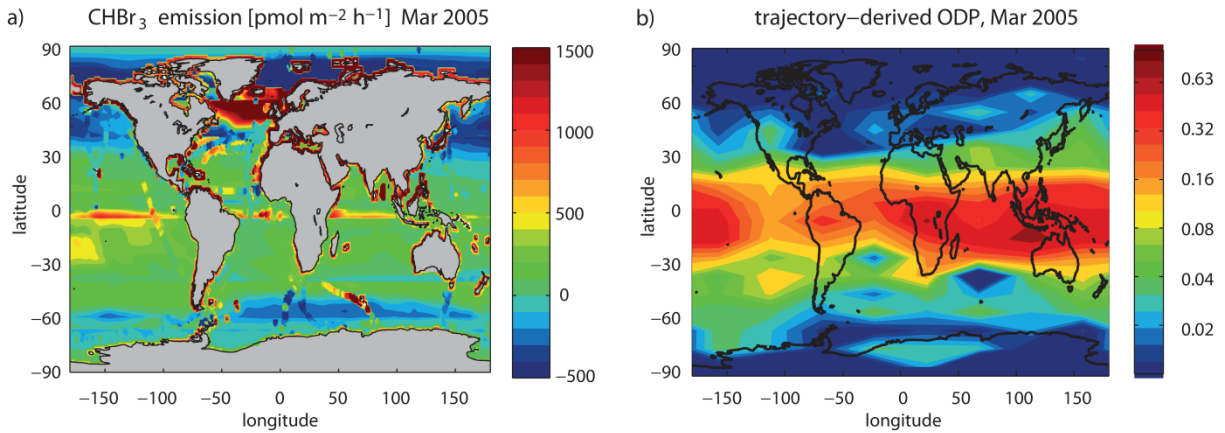
- 885
- 886 Hossaini, R., M. P. Chipperfield, S. Dhomse, C. Ordóñez, A. Saiz-Lopez, N. L. Abraham, A.
887 Archibald, P. Braesicke, P. Telford, and N. Warwick: Modelling future changes to the
888 stratospheric source gas injection of biogenic bromocarbons, *Geophys. Res. Lett.*, 39,
889 L20813, doi:10.1029/2012GL053401, 2012.
- 890
- 891 Hossaini, R., Mantle, H., Chipperfield, M. P., Montzka, S. A., Hamer, P., Ziska, F., Quack,
892 B., Krüger, K., Tegtmeier, S., Atlas, E., Sala, S., Engel, A., Bönisch, H., Keber, T., Oram, D.,
893 Mills, G., Ordóñez, C., Saiz-Lopez, A., Warwick, N., Liang, Q., Feng, W., Moore, F., Miller,
894 B. R., Marécal, V., Richards, N. A. D., Dorf, M., and Pfeilsticker, K.: Evaluating global
895 emission inventories of biogenic bromocarbons, *Atmos. Chem. Phys.*, 13, 11819-11838,
896 doi:10.5194/acp-13-11819-2013, 2013.
- 897
- 898 Hossaini, R., M. P. Chipperfield, S. A. Montzka, A. Rap, S. Dhomse, and W. Feng:
899 Efficiency of short-lived halogens at influencing climate through depletion of stratospheric
900 ozone, *Nature Geosci.*, 8(3), 186–190, doi:10.1038/ngeo2363, 2015.
- 901
- 902 Leedham, E. C., C. Hughes, F. S. L. Keng, S.-M. Phang, G. Malin, and W. T. Sturges:
903 Emission of atmospherically significant halocarbons by naturally occurring and farmed
904 tropical macroalgae, *Biogeosciences*, 10, 3615–3633, doi:10.5194/bg-10-3615-2013, 2013.
- 905
- 906 Kay, J. E., et al.: Exposing global cloud biases in the Community Atmosphere Model (CAM)
907 using satellite observations and their corresponding instrument simulators, *J. Climate*, 25,
908 5190–5207, 2012.
- 909
- 910 Krüger, K., Tegtmeier, S., and Rex, M.: Long-term climatology of air mass transport through
911 the Tropical Tropopause Layer (TTL) during NH winter, *Atmos. Chem. Phys.*, 8, 813-823,
912 doi:10.5194/acp-8-813-2008, 2008.
- 913
- 914 Liang, Q., Stolarski, R. S., Kawa, S. R., Nielsen, J. E., Douglass, A. R., Rodriguez, J. M.,
915 Blake, D. R., Atlas, E. L., and Ott, L. E.: Finding the missing stratospheric Br_y: a global
916 modeling study of CHBr₃ and CH₂Br₂, *Atmos. Chem. Phys.*, 10, 2269-2286, doi:10.5194/acp-
917 10-2269-2010, 2010.
- 918

- 919 Liang, Q., Atlas, E., Blake, D., Dorf, M., Pfeilsticker, K., and Schauffler, S.: Convective
920 transport of very short lived bromocarbons to the stratosphere, *Atmos. Chem. Phys.*, 14, 5781-
921 5792, doi:10.5194/acp-14-5781-2014, 2014.
922
- 923 ~~Montzka, S., et al.: Ozone depleting substances (ODSs) and related chemicals, in Scientific
924 Assessment of Ozone Depletion: 2010, Rep. 52, chap. 1, pp. 1–112, Global Ozone Res. and
925 Monit. Proj., World Meteorol. Organ., Geneva, Switzerland, 2011.~~
926
- 927 Neale, R. B., J. H. Richter, and M. Jochum: The impact of convection on ENSO: From a
928 delayed oscillator to a series of events. *J. Climate*, 21, 5904–5924, 2008.
929
- 930 Neale, R. B., and Coauthors: Description of the NCAR Community Atmosphere Model
931 (CAM5.0). NCAR Tech. Rep. NCAR/TN-486+STR, 268 pp, 2010.
932
- 933 Neely, R. R., Toon, O. B., Solomon, S., Vernier, J. P., Alvarez, C., English, J. M., Rosenlof,
934 K. H., Mills, M. J., Bardeen, C. G., Daniel, J. S. and Thayer, J. P.: Recent anthropogenic
935 increases in SO₂ from Asia have minimal impact on stratospheric aerosol, *Geophys. Res.
936 Lett.*, 40(5), 999–1004, doi:10.1002/grl.50263, 2013.
937
- 938 Nightingale, P. D., Malin, G., Law, C. S., Watson, A. J., Liss, P. S., Liddicoat, M. I., Boutin,
939 J. and Upstill-Goddard, R. C.: In situ evaluation of air-sea gas exchange parameterizations
940 using novel conservative and volatile tracers, *Global Biogeochemical Cycles*, 14(1), 373–387,
941 doi:10.1029/1999GB900091, 2000.
942
- 943 Phang, S.-M., Yeong, H.-Y., Lim, P.-E., Nor, A. R., and Gan, K. T.: Commercial varieties of
944 *Kappaphycus* and *Eucheuma* in Malaysia, *Malaysian J. Sci.*, 29, 214–224, 2010.
945
- 946 Pisso, I., Haynes, P. H., and Law, K. S.: Emission location dependent ozone depletion
947 potentials for very short-lived halogenated species, *Atmos. Chem. Phys.*, 10, 12025-12036,
948 doi:10.5194/acp-10-12025-2010, 2010.
949
- 950 Pyle, J. A., N. Warwick, X. Yang, P. J. Young, and G. Zeng: Climate/chemistry feedbacks
951 and biogenic emissions, *Philos. Trans. R. Soc. A*, 365(1856), 1727–1740,
952 doi:10.1098/rsta.2007.2041, 2007.

- 953
- 954 Quack, B., E. Atlas, G. Petrick, and D. W. R. Wallace: Bromoform and dibromomethane
955 above the Mauritanian upwelling: Atmospheric distributions and oceanic emissions, J.
956 Geophys. Res., 112(D9), D09312, doi:10.1029/2006JD007614, 2007.
- 957
- 958 Ravishankara, A.R., J. S. Daniel, R. W. Portmann: Nitrous oxide (N_2O): The dominant ozone-
959 depleting substance emitted in the 21st century. *Science* 326:123–125, 2009.
- 960
- 961 Rybka, H., and H. Tost: Uncertainties in future climate predictions due to convection
962 parameterizations, *Atmospheric Chemistry and Physics*, 14(11), 5561–5576, doi:10.5194/acp-
963 14-5561-2014, 2014.
- 964
- 965 Sala, S., Bönisch, H., Keber, T., Oram, D. E., Mills, G., and Engel, A.: Deriving an
966 atmospheric budget of total organic bromine using airborne in situ measurements from the
967 western Pacific area during SHIVA, *Atmos. Chem. Phys.*, 14, 6903-6923, doi:10.5194/acp-
968 14-6903-2014, 2014.
- 969
- 970 Salawitch, R. J., Weisenstein, D. K., Kovalenko, L. J., Sioris, C. E., Wennberg, P. O., Chance,
971 K., Ko, M. K. W., and McLinden, C. A.: Sensitivity of ozone to bromine in the lower
972 stratosphere, *Geophys. Res. Lett.*, 32, L05811, doi:10.1029/2004GL021504, 2005.
- 973
- 974 Schofield, R., S. Fueglistaler, I. Wohltmann, and M. Rex: Sensitivity of stratospheric Bry to
975 uncertainties in very short lived substance emissions and atmospheric transport, *Atmos Chem
976 Phys.*, 11(4), 1379–1392, doi:10.5194/acp-11-1379-2011, 2011.
- 977
- 978 Sinnhuber, B.-M., Sheode, N., Sinnhuber, M., Chipperfield, M. P., and Feng, W.: The
979 contribution of anthropogenic bromine emissions to past stratospheric ozone trends: a
980 modelling study, *Atmos. Chem. Phys.*, 9, 2863-2871, doi:10.5194/acp-9-2863-2009, 2009.
- 981
- 982 Sioris, C. E., et al.: Latitudinal and vertical distribution of bromine monoxide in the lower
983 stratosphere from Scanning Imaging Absorption Spectrometer for Atmospheric Chartography
984 limb scattering measurements, *J. Geophys. Res.*, 111, D14301, doi: 10.1029/2005JD006479,
985 2006.
- 986

- 987 Solomon, S., M. Mills, L. E. Heidt, W. H. Pollock, and A. F. Tuck: On the evaluation of
988 ozone depletion potentials, *J. Geophys. Res.*, 97, 825–842, 1992.
- 989
- 990 Tang, Q., Zhang, J., and Fang, J.: Shellfish and seaweed mariculture increase atmospheric
991 CO₂ absorption by coastal ecosystems, *Mar. Ecol.-Prog. Ser.*, 424, 97–104, 2011.
- 992
- 993 Taylor, K. E., R. J. Stouffer, and G. A. Meehl: The CMIP5 experiment design. *Bull. Amer.*
994 *Meteor. Soc.*, **93**, 485–498, 2012.
- 995
- 996 Tegtmeier, S., Krüger, K., Quack, B., Atlas, E. L., Pisso, I., Stohl, A. and Yang, X.: Emission
997 and transport of bromocarbons: from the West Pacific ocean into the stratosphere,
998 *Atmospheric Chemistry and Physics*, 12(22), 10633–10648, doi:10.5194/acp-12-10633-2012,
999 2012.
- 1000
- 1001 Tilmes, S., D. E. Kinnison, R. R. Garcia, R. Salawitch, T. Carty, J. Lee-Taylor, S. Madronich,
1002 and K. Chance (2012), Impact of very short-lived halogens on stratospheric ozone abundance
1003 and UV radiation in a geo-engineered atmosphere, *Atmospheric Chemistry and Physics*,
1004 12(22), 10945–10955.
- 1005
- 1006 Velders, G. J. M., S. O. Andersen, J. S. Daniel, D. W. Fahey and M. McFarland: The
1007 Importance of the Montreal Protocol in Protecting Climate, *PNAS*, 104:4814 – 4819, doi:
1008 10.1073/pnas.0610328104, 2007.
- 1009
- 1010 Vernier, J.-P., et al., Major influence of tropical volcanic eruptions on the stratospheric
1011 aerosol layer during the last decade, *Geophys. Res. Lett.*, 38, L12807,
1012 doi:10.1029/2011GL047563, 2011.
- 1013 Warwick, N. J., J. A. Pyle, G. D. Carver, X. Yang, N. H. Savage, F. M. O'Connor, and R. A.
1014 Cox: Global modeling of biogenic bromocarbons, *J. Geophys. Res.*, 111, D24305,
1015 doi:10.1029/2006JD007264, 2006.
- 1016
- 1017 Wuebbles, D. J.: Chlorocarbon emission scenarios: Potential impact on stratospheric ozone,
1018 *J. Geophys. Res.*, 88, 1433–1443, 1983.
- 1019

- 1020 Wuebbles, D. J., K. Patten, M. Johnson, and R. Kotamarthi: New methodology for ozone
1021 depletion potentials of short-lived compounds: n-propyl bromide as an example, *J. Geophys.*
1022 *Res.*, 106, 14551–14571, 2001.
1023
- 1024 Yang, X., Abraham, N. L., Archibald, A. T., Braesicke, P., Keeble, J., Telford, P. J.,
1025 Warwick, N. J., and Pyle, J. A.: How sensitive is the recovery of stratospheric ozone to
1026 changes in concentrations of very short-lived bromocarbons?, *Atmos. Chem. Phys.*, 14,
1027 10431-10438, doi:10.5194/acp-14-10431-2014, 2014.
1028
- 1029 Ziska, F., Quack, B., Abrahamsson, K., Archer, S. D., Atlas, E., Bell, T., Butler, J. H.,
1030 Carpenter, L. J., Jones, C. E., Harris, N. R. P., Hepach, H., Heumann, K. G., Hughes, C.,
1031 Kuss, J., Krüger, K., Liss, P., Moore, R. M., Orlikowska, A., Raimund, S., Reeves, C. E.,
1032 Reifenhäuser, W., Robinson, A. D., Schall, C., Tanhua, T., Tegtmeier, S., Turner, S., Wang,
1033 L., Wallace, D., Williams, J., Yamamoto, H., Yvon-Lewis, S., and Yokouchi, Y.: Global sea-
1034 to-air flux climatology for bromoform, dibromomethane and methyl iodide, *Atmos. Chem.*
1035 *Phys.*, 13, 8915-8934, doi:10.5194/acp-13-8915-2013, 2013.
1036
- 1037 Ziska, F., Quack, B., Krüger, K., and Tegtmeier, S.: Future emissions of halocarbons based on
1038 CMIP 5 model output fields, to be submitted to ACPD.
1039
- 1040
- 1041
- 1042
- 1043
- 1044
- 1045
- 1046
- 1047



1048

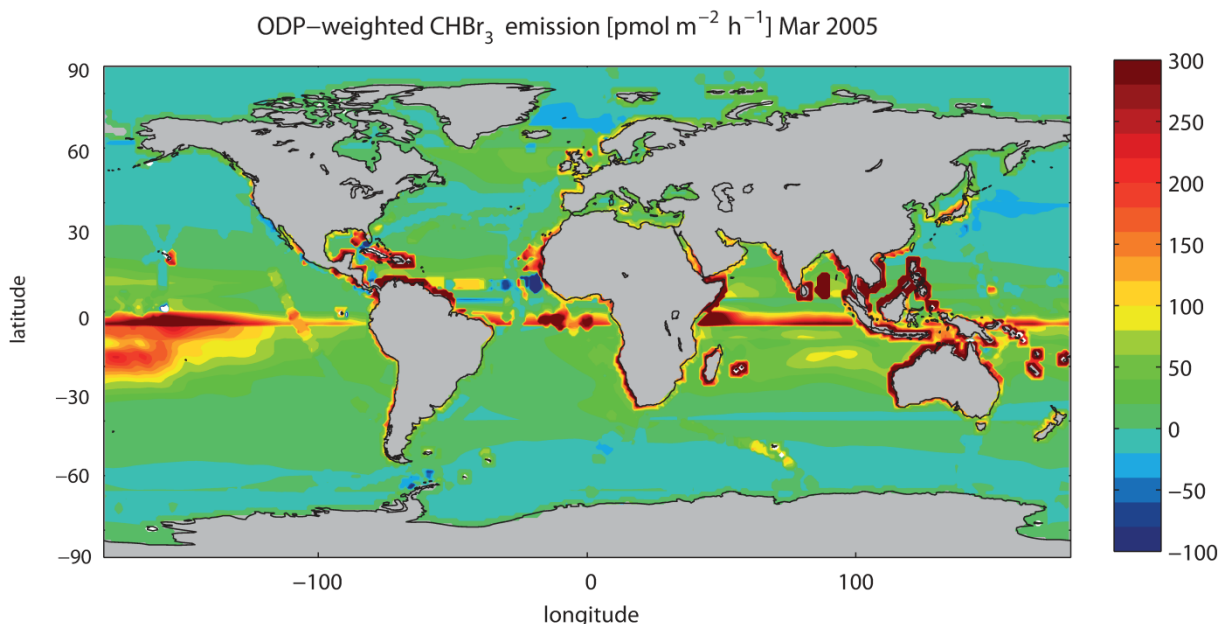
1049

1050 **Figure 1.** Global CHBr₃ emissions (a) and ODP (b) are given for March 2001. The CHBr₃ emissions
 1051 are bottom-up estimates based on the extrapolation of in-situ measurements (Ziska et al., 2013). The
 1052 ODP is given as a function of time and location of emission and was derived based on a Langrangian
 1053 approach (Pisso et al., 2010).

1054

1055

1056



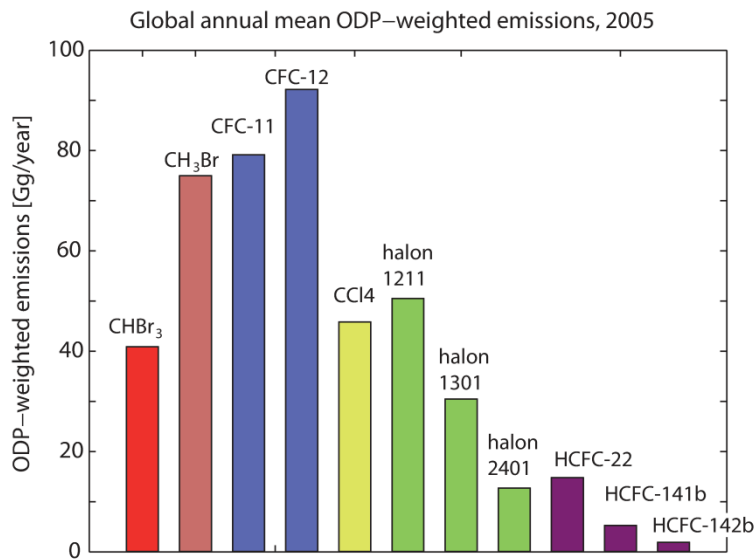
1057

1058 **Figure 2.** Global ODP-weighted CHBr₃ emissions are given for March 2005. The ODP-weighted
 1059 emissions have been calculated by multiplying the CHBr₃ emissions with the ODP at each grid point.

1060

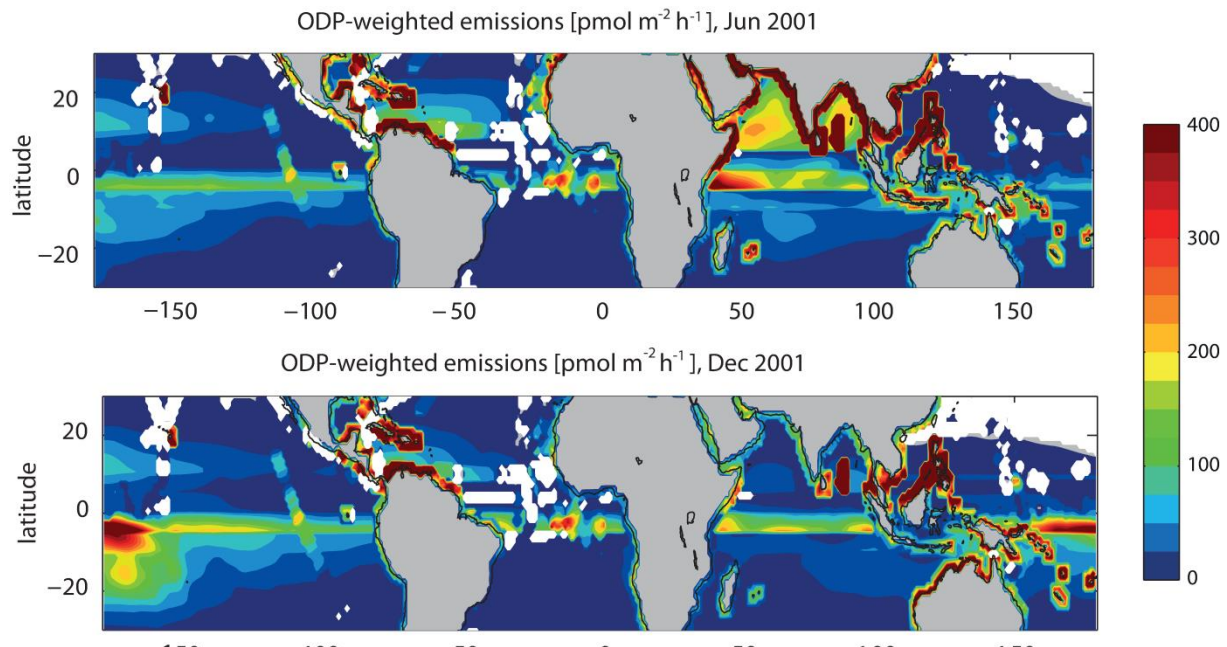
1061

1062



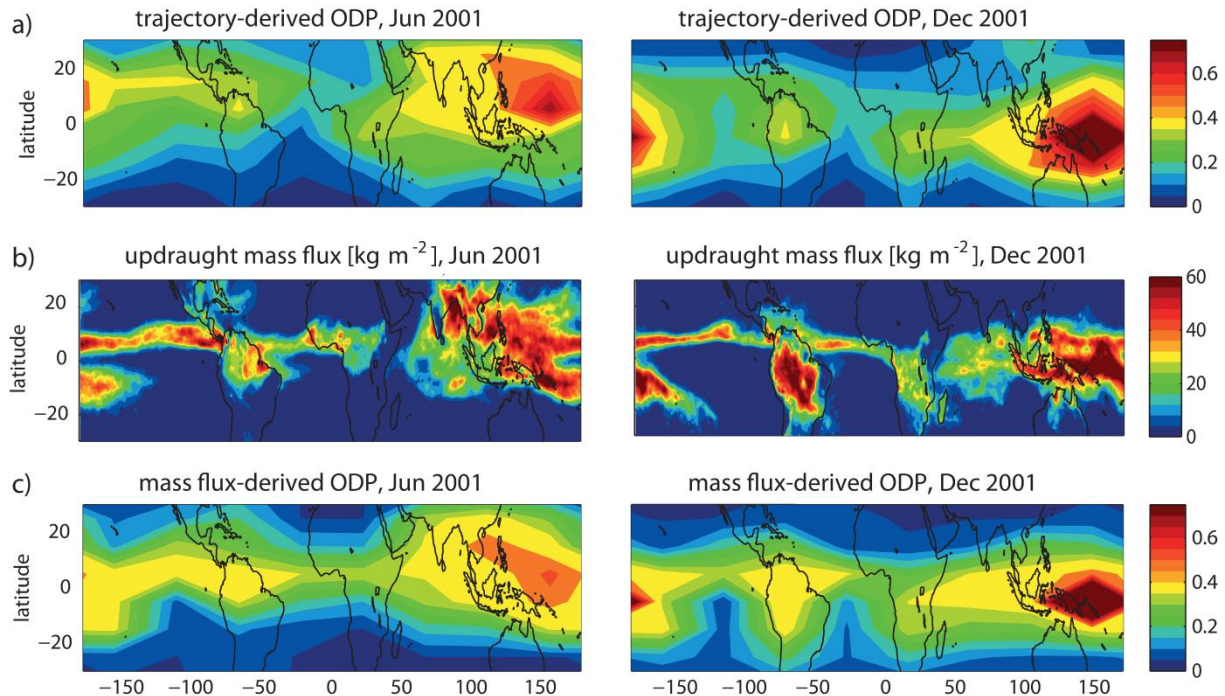
1063
1064 **Figure 3.** A comparison of the global annual mean ODP-weighted emissions of CHBr₃ and long-lived
1065 halocarbons is shown for 2005. Emissions of long-lived halocarbons being derived from NOAA and
1066 AGAGE global sampling network measurements (Montzka et al., 2011).

1067
1068
1069



1072 **Figure 4.** ODP-weighted emissions calculated as the product of the emissions maps (Figure S1 in the
1073 Supplement) and the trajectory-based ODP fields (Figure 5a) are displayed for June and December
1074 2001.

1075
1076

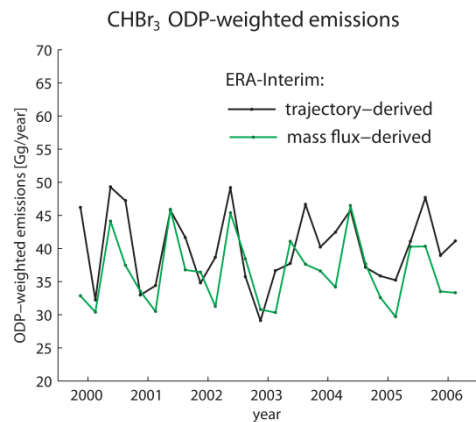


1077

Figure 5. Trajectory-based CHBr₃ ODP fields (a), monthly mean ERA-Interim updraught mass flux between 250 and 80 hPa (b), and the mass flux-derived ODP (c) are displayed for June and December 2001.

1081

1082



1083

Figure 6. Time series of ODP-weighted CHBr₃ emissions based on ERA-Interim trajectory-derived ODP (black line) and mass flux-derived ODP (green line) for March, June, September and December 1999 to 2006.

1087

1088

CHBr₃ ODP-weighted emissions (ERA-Interim)

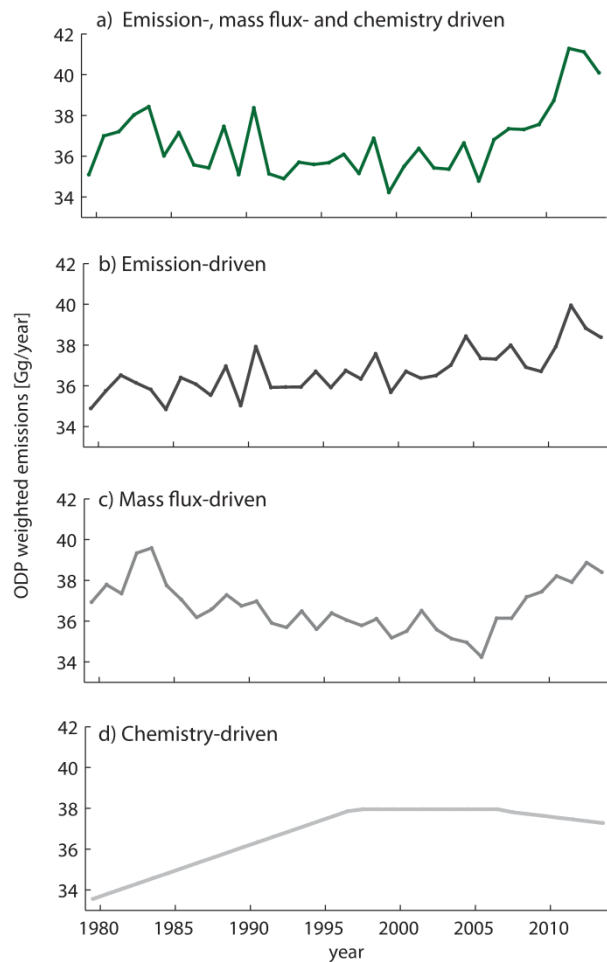


Figure 7. Time series of ODP-weighted CHBr₃ emissions for 1979-2013 based on ERA-Interim mass flux-derived ODP is shown (a). Additionally, sensitivity studies are displayed where two factors are kept constant at their respective 1979-2013 mean values, while the other factor varies with time. The sensitivity studies include ODP-weighted CHBr₃ emissions driven by time-varying emissions (b), time-varying mass flux-derived ODP (c), and time-varying stratospheric chemistry (d).

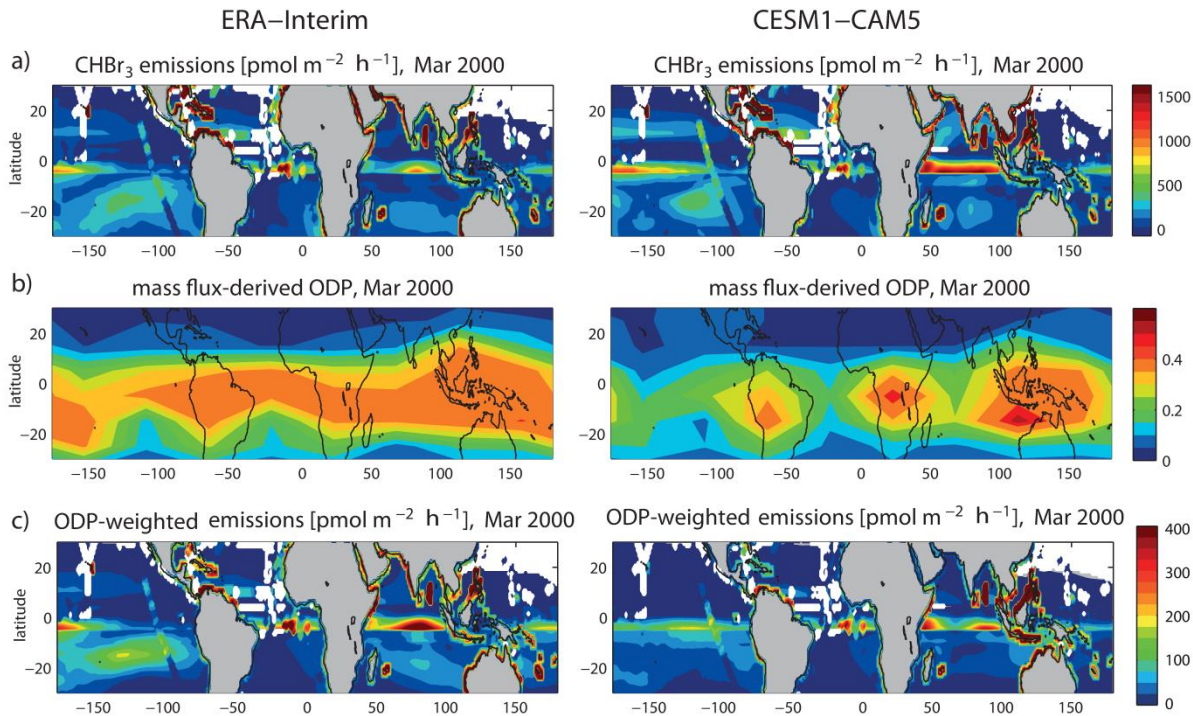
1089

1090 **Figure 7.** Time series of ODP-weighted CHBr₃ emissions for 1979-2013 based on ERA-Interim mass
1091 flux-derived ODP is shown (a). Additionally, sensitivity studies are displayed where two factors are
1092 kept constant at their respective 1979-2013 mean values, while the other factor varies with time. The
1093 sensitivity studies include ODP-weighted CHBr₃ emissions driven by time-varying emissions (b),
1094 time-varying mass flux-derived ODP (c), and time-varying stratospheric chemistry (d).

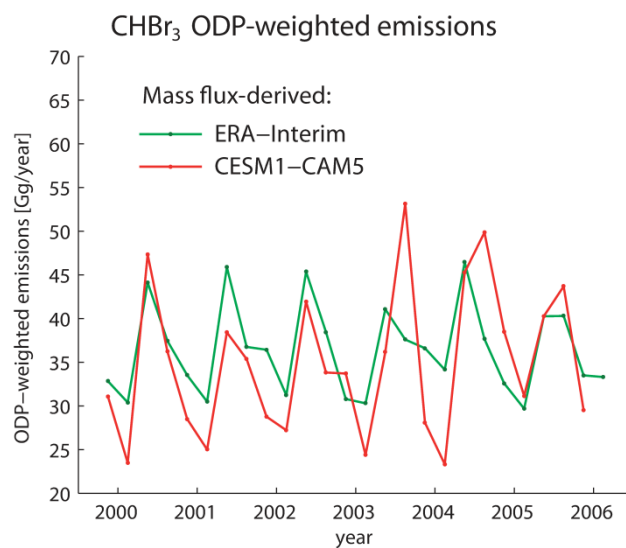
1095

1096

1097



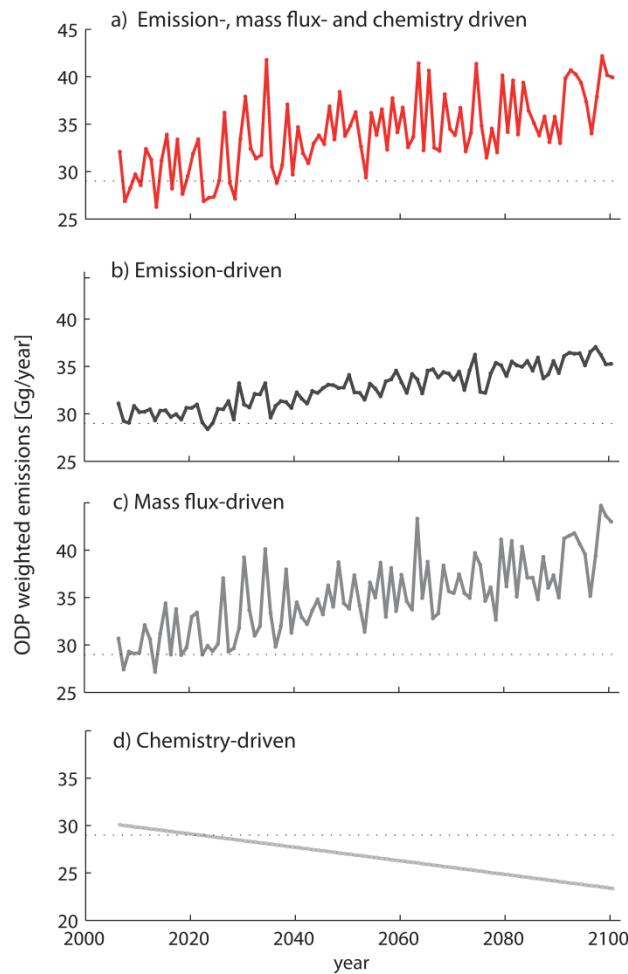
1098
1099
1100
1101
1102
1103



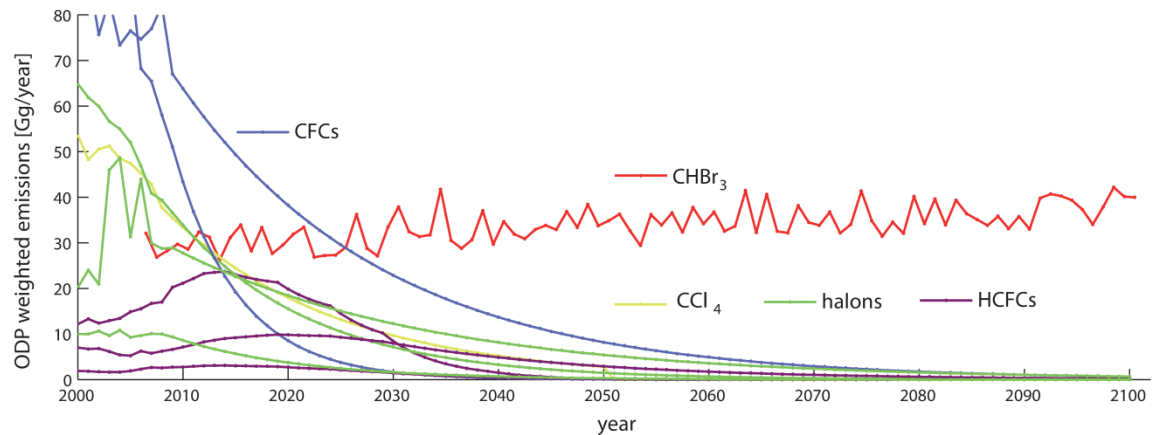
1104
1105
1106
1107
1108
1109
1110

Figure 9. Time series of CHBr₃ ODP-weighted emissions based on ERA-Interim (green line) and on historical CESM1-CAM5 runs (red line) are shown. The ODP is calculated from the updraught mass flux fields.

CHBr₃ ODP-weighted emissions (CESM1-CAM5)



1111
1112
1113 **Figure 10.** Time series of CHBr₃ ODP-weighted emissions for 2006-2100 based on future (RCP 8.5
1114 scenario) CESM1-CAM5 runs are shown (a). Additionally, the future time series are displayed with
1115 two factors kept constant at their respective 2006-2015 mean value while the other factor varies with
1116 time. The sensitivity studies include ODP-weighted CHBr₃ emissions driven by time-varying
1117 emissions (b), time-varying mass flux-derived ODP (c), and time-varying stratospheric chemistry (d).
1118
1119
1120



1121
 1122 **Figure 11:** Future projections of annual mean ODP-weighted emissions of CHBr_3 and other long-lived
 1123 halocarbons are shown for 2000-2100. Future ODP-weighted emission estimates for long-lived
 1124 halocarbons (halons: halon 1211, 1301, 2402; HCFCs: HCFC-22, -141, -142) are shown.

1125
 1126
 1127
 1128
 1129